Beneficial effects of voluntary exercise therapy on an Alzheimer's mouse model are dependent on aquaporin 4-mediated glymphatic transport

Yun Liu
Nanjing Medical University
Weixi Feng
Nanjing Medical University
Panpan Hu
Nanjing Medical University
Shuang Zhai
Nanjing Medical University
Rui Zhang
Nanjing Medical University
Qian Li
Nanjing Medical University
Charles Marsahall
Nanjing Medical University
Ming Xiao (mingx@njmu.edu.cn)
Nanjing Medical University https://orcid.org/0000-0001-5528-9102
Ting Wu
Nanjing Medical University

Research

Keywords: Alzheimer's disease, astrocytes, aquaporin-4, glymphatic system, voluntary exercise

Posted Date: November 16th, 2020

DOI: https://doi.org/10.21203/rs.3.rs-108136/v1

Abstract

Background: Epidemiological and clinical evidence suggest there is an effective time window for the ability of exercise to slow the progression of Alzheimer's disease (AD). Astrocyte aquaporin-4 (AQP4) dependent glymphatic transport is necessary for clearance of extracellular amyloid-β (Aβ) from the brain. The purpose of this study is to explore whether this Aβ clearance mechanism is involved in the time-dependent benefit of exercise on Aβ related pathology.

Method: 3- and 7-month-old male wild type (WT) mice, $APP695_{swe}$/PS1-dE9 (APP/PS1) mice and AQP4 knockout ($AQP4^{-/-}$)/APP/PS1 mice received voluntary wheel exercise intervention for 2 months, followed by behavioral and pathological analyses.

Results: 9-month-old APP/PS1 mice showed enhanced reactive astrogliosis, accompanied with widespread loss of perivascular AQP4 polarization, when compared to 5-month-old APP/PS1 mice. Voluntary exercise improved AQP4 polarity and glymphatic transport, reduced glial inflammation and brain Aβ plaque load, plus alleviated synapse protein loss and cognitive deficits in 5-month-old, but not 9-month-old, APP/PS1 mice. Exercise intervention did not mitigate glymphatic transport dysfunction, Aβ accumulation and cognitive impairment in $AQP4^{-/-}$/APP/PS1 mice at 5 or 9 months of age.

Conclusion: These results have revealed that AQP4-dependent glymphatic transport is an influential factor in the timeliness of voluntary exercise ability to alleviate Aβ pathology, potentially offering a new target for the early prevention of the disease.

Background

Alzheimer's disease (AD) is a common neurodegenerative disease, characterized by extracellular amyloid-β (Aβ) plaques in the brain [1]. Currently, non-pharmacological interventions are receiving substantial interest due to the inability to develop AD therapeutic drugs and vaccines [2]. Epidemiological and clinical studies show that physical activity improves cognition during healthy aging [4–6], as well as individuals with mild cognitive impairment [7–9]. However, exercise therapy has not been shown to exert explicitly beneficial outcomes on patients with AD [10, 11]. Exploring the underlying mechanisms for an effective exercise intervention time window is crucial for the prevention of AD.

Experimental animal studies indicate that exercise plays a variety of neuroprotective roles, including promoting neurogenesis, reducing neuroinflammation, improving mitochondrial energy metabolism and promoting neurotrophic factor secretion [12, 13]. Notably, both voluntary exercise and forced exercise have been shown to reduce extracellular Aβ levels in the brains of several transgenic mouse models of AD [14–17]. However, there is considerable evidence that exercise interventions do not reduce Aβ plague load in mice with mid- to late-stage AD-like pathology [18–21]. The mechanism for exercise promoting Aβ clearance within an effective time window remains unclear.

A variety of clearance pathways are implicated in removal of extracellular Aβ from the brain, which include enzymatic degradation, cellular uptake and transport across the brain barriers [22]. Recent findings suggest that the glymphatic system may be a large contributor in extracellular Aβ clearance [23]. The glymphatic system, also known as the perivascular space, is surrounded by incomplete continuous astrocyte endfeet, at which large amounts of aquaporin 4 (AQP4) is located [24]. Such structural features facilitate rapid removal of brain interstitial fluid and soluble macromolecular substances from the brain [25]. Aged mice, as well as mouse models of AD, show loss of specific localization of AQP4 in perivascular endfeet due to reactive astrogliosis, which in turn impairs glymphatic clearance of Aβ [26, 27]. Our previous studies reported that deletion of AQP4 increases Aβ plaque deposit and cerebral amyloid angiopathy in 12-month-old APP/PS1 mice [28]. Moreover, recent studies have shown that voluntary exercise promotes glymphatic clearance of Aβ, which is associated with improved astrocytic AQP4 polarization in aged mice [29]. Together, these findings suggest that AQP4-mediated glymphatic clearance of Aβ may act as a key factor in determining a therapeutic time window for exercise in AD. In particular, under healthy aging or the onset stage of AD, exercise facilitates clearance of Aβ from the brain parenchyma via increased AQP4 dependent bulk flow along the glymphatic pathway. However, with the progress of AD, the polarity of AQP4 is totally impaired because of reactive astrogliosis. Therefore, the structural basis for exercise improving glymphatic clearance is elapsed, subsequently failing to prevent Aβ-related pathological cascades.

APP695swe/PS1-dE9 (APP/PS1) mice are extensively used mouse model of AD with occurrence of Aβ-associated long-term memory malfunction from approximately 6–7 months of age, which serves as a hallmark of moderate stage AD [30]. At 3 months old, despite no Aβ plaques, this AD mouse line exhibits a mild activation of astrocytes with slight impairments of AQP4 polarity and glymphatic transport [31, 32]. Therefore, we chose the 3- and 7-month-old APP/PS1 mice and AQP4$^{-/-}$/APP/PS1 mice to test whether the time-dependent benefit of exercise on Aβ related pathology is dependent on AQP4-mediated glymphatic transport.

Materials And Methods

Animals

AQP4$^{-/-}$/APP/PS1 mice were established via AQP4$^{-/-}$ mice crossing with APP695/PS1-dE9 mice as described previously [28]. Both 3-month-old and 7-month-old male AQP4$^{-/-}$/APP/PS1 mice, APP/PS1 mice and their wild-type (WT) littermates were randomly divide into exercise group and sedentary group, respectively, and received 2-month voluntary exercise treatment followed by behavioral tests (Fig. 1A). The animal experiments were approved by the Animal Ethical and Welfare Committee of Nanjing Medical University.

Voluntary exercise

Mice habituated for one week prior to the beginning of voluntary exercise training, referred to as the “pre-intervention” period. Exercise mice were placed in the running wheel for 4 h every day, 5 days per week, for

2 months. Control mice were placed in the same room as the exercise mice.

Y-maze test

The Y-maze test was carried out to evaluate short-term working memory [28]. It consisted of 2 trials with a 1-h interval. Three identical arms of the maze were randomly designated start arm, novel arm, and other arm. In the first trial, one arm of the Y-maze was blocked by a removable door, and the animal was placed in the start arm and allowed to explore the two arms for 5 min. In the second trial, the blocking baffle was removed and mice could now have access to all three arms for 5 min. The number of entries into the novel arm, and the percentage of novel arm entries made during the second trial, were analyzed.

Novel object recognition test (NORT)

The NORT was performed to assess object recognition memory [33]. This task consisted of two trials, with an interval of 2 hours. In the first trial, mice were placed in an arena with two of the same objects and allowed to explore for 5 min. Following a two-hour delay, mice were placed back in the familiar arena where a novel object was replaced by one of the identical objects (the other object remained the same), and mice were allowed to freely re-explore for 5 min. Time spent exploring the familiar and novel objects were recorded. The discrimination index was derived by calculating the time spent exploring the novel object/the time spent exploring novel object + the time spent exploring a familiar object.

Morris water maze (MWM) test

The MWM task was performed to assess spatial learning and memory function [28]. Briefly, the mice received 6 days of training and a probe test on the 7th day. In the training trail, mice were given as long as 60 s to find the dark-colored cylindrical platform submerged 1 cm beneath the surface of water which was made opaque with milk and invisible to the mice, and required to remain seated on the platform for 5 s. Mice underwent four trials per day, starting from each of four different locations in the pool. The escape latency and swimming speed were analyzed. During the probe trail, the platform was removed from the pool and mice were allowed to swim in the pool for 60 s in order to determine the percentage of total time spent in each quadrant and the number of crossing where the platform was located.

Cisterna magna injection of fluorescent tracer

Cisterna magna injection of fluorescent tracer was performed as described previously [24, 31]. The mice were anesthetized and positioned in a stereotaxic apparatus while the posterior atlanto-occipital membrane was surgically exposed. 5 μl Texas Red-dextran-3 (TR-d3, 3000 MW; Invitrogen, Cat. D3328) was injected at a concentration of 0.5 mg/mL into the cisterna magna by a microsyringe needle at a flow rate of 1 μl/min. Forty minutes after the start of infusion, animals were anesthetized again. The brains were removed and post-fixed overnight in 4% paraformaldehyde (PFA) at 4 °C.

Tissue preparation

Following behavioral testing, mice were anesthetized and perfused transcardially with 0.9% saline from the left ventricle by a perfusion pump (Longer Pump, China, Cat # BT100-2J). The entire brain was carefully removed from the skull and divided into two hemispheres. One hemisphere was postfixed in 4% PFA at 4 °C overnight and subsequently dehydrated in a series of graded ethanol solutions. The brains

were embedded in paraffin and cut into 5-μm thick sagittal sections using a microtome (Leica, Germany Cat. # RM2135). Serial sections containing the hippocampus and cerebral cortex were placed on gelatin-coated slides for immunohistochemistry. The other hemisphere was immediately frozen in liquid nitrogen and then stored at -80 °C until Western blot or ELISA analyses. For CSF tracer experiments, PFA postfixed forebrain tissues were sliced with a vibrating microtome (Word Precision Instruments Inc, WPI, USA; Cat. NVSLM1), at a thickness of 100 μm, and mounted onto gelatin-coated slides in sequence.

Immunohistochemistry

Brain sections were deparaffinized, hydrated and microwaved in citric acid buffer to achieve antigen retrieval, then treated with 3% H_2O_2 for 20 min in order to reduce endogenous peroxidase activity. Brain sections were incubated with following primary antibodies directed against glial fibrillary acidic protein (GFAP) (1:1000; Millipore; Cat. MAB360), AQP4 (1:400; Millipore; Cat. AB3594), 6E10 (1:1000; Covance, Cat. 803001), ionized calcium binding adaptor molecule 1 (Iba-1) (1:1000; Wako, Cat. 019-19741), postsynaptic density protein 95 (PSD-95) (1:200; Abcam, Cat. ab18258) and synaptophysin (SYN) (1:200, Abcam, Cat. ab64581) at 4 °C overnight. The next day, sections were incubated for 1 hour at room temperature with secondary antibodies labeled with horseradish peroxidase and developed with a diaminobenzidine (DAB) horseradish peroxidase color development kit (Sigma-Aldrich, Cat. D8001). Partial AQP4 stained sections were counterstained with Congo red (Sigma-Aldrich, Cat. C6767).

Immunofluorescence

Brain sections were blocked for 1 hour at room temperature with 5% BSA and incubated with the primary antibodies including mouse anti-GFAP (1:1000) and rabbit anti-AQP4 (1:400) at 4 °C overnight. The next day, all sections were rinsed 3 times and incubated for 2 hours at room temperature in a mixture of Alexa Flour™ 555 donkey anti-mouse IgG (1:1000; Thermo Fisher; Cat. A31570) and Alexa Flour™ 488 donkey anti-rabbit IgG (1:1000; Thermo Fisher; Cat. A21206). After rinsing, the sections were incubated for 6 min in 4’,6-diamidino-2-phenylindole (DAPI) (1:1000; Thermo Fisher; Cat. D21490) and coverslipped with anti-fluorescent quencher.

Thioflavine-S staining

Deparaffinized sections were incubated with 1% thioflavine-S (Sigma-Aldrich) for 5 min. Next, 70% ethanol was used to differentiate for 5 min, followed by rinsing with distilled water. The brain sections coverslipped with anti-fluorescent quencher.

Image analysis

Brain sections were captured by a digital microscope (Leica Microsystems, Wetzlar, Germany) with constant exposure time, offset, and gain for each staining marker. The positive signal area was measured with Image J (NIH). The positive signal percentage area of GFAP, Ibal, 6E10 and AQP4 was calculated by dividing the area of positive signal to the total area in the hippocampus and adjacent cortex. The mean integrated optical density (MIOD = IOD/total area) was measured to assess immunostaining intensity of SYN and PSD-95 in the hippocampus. For analysis of AQP4 polarization, images at 400 × magnification were randomly captured from the superficial layers of the frontal cortex. The mean immunofluorescent or

immunohistochemical intensity of AQP4 at the regions immediately abutting vessels or pia maters and adjacent parenchyma domains was measured. AQP4 polarization was calculated by comparing expression ratios of AQP4 at perivascular domains or abutting pia maters versus adjacent parenchymal domains [23, 28]. For the analysis of intracisternally injected TR-d3 diffused into the brain parenchyma, positive signal percentage area of TR-d3 was measured on 3 coronal sections at + 0.86, 0 and − 1.06 mm from anterior to posterior, relative to the bregma. TR-d3 penetration along perivascular spaces was quantified on 400 × magnification images of the frontal cortex (Fig. 2A). The fluorescence intensity within the perivascular space was measured along microvessels (diameter = 30–50 μm) extending 250 μm below the brain surface. All quantification was done blind to animal genotype and treatment.

Western blotting

Hippocampal tissues were homogenized at 4 °C, then centrifuged at 12,000 rpm for 15 min. The extracts were loaded onto 10%-12% Tris SDS gels and transferred onto polyvinylidene fluoride membranes. After blocking by 5% skim milk diluted with TBST buffer for 1 h, these membranes were incubated at 4 °C overnight with one of the following primary antibodies: $A\beta_{1-40}$ (1:1000, Abcam, Cat. ab20068), $A\beta_{1-42}$ (1:1000, Abcam, Cat. ab201060), SYN (1:1500, Abcam, Cat. ab64581), PSD-95 (1:1000; Abcam, Cat. ab18258), brain-derived neurotrophic factor (BDNF) (1:1000; Abcam, Cat. Ab108319), tropomyosin receptor kinase B (TrkB) (1:1000; Abcam, ab187041), cyclic adenosine monophosphate response element binding protein (CREB) (1:1000; CST, Cat. 9197S), p-CREB (1:1000; CST, Cat. 9198S) and glyceraldehyde-3-phosphate dehydrogenase (GAPDH) (1:3000; Bioworld, Cat. BS60630). Following TBST washing, the membranes were incubated with horseradish peroxidase-labeled secondary antibodies (1:2000; ZSGB-BIO; Cat. ZB2301, Cat. ZB2302) for 1 h at room temperature. The protein bands were visualized via ECL plus detection system. GAPDH was used as loading control.

ELISA

The frontal cortex were homogenized in TBS with protease inhibitors and 1% Triton X-100, followed by centrifugation at 20,000 × g for 1 h. Supernatants were set aside for measurements utilizing soluble $A\beta_{1-40}$ (R&D Systems; Cat. DAB140B), $A\beta_{1-42}$ (R&D Systems; Cat. DAB142), interleukin 1 beta (IL-1β) (Excell Biotech Corporation; Cat. EM001-96), interleukin 6 (IL-6) (Excell Biotech Corporation; Cat. EM004-96) and tumor necrosis factor-α (TNF-α) (Excell Biotech Corporation; Cat. EM008-96). The above indexes were quantified with corresponding ELISA kits according to the manufacturer's instructions.

Statistical analysis

All data were expressed as means ± SEM. Using GraphPad Prism, version 5.02 software (GraphPad software, San Diego, CA, USA), data for the MWM platform training and TR-d3 diffusion within the perivascular space, were analyzed by repeated-measures analysis of variance (ANOVA). Other data were analyzed by Student's t test, two-way ANOVA and multi-way ANOVA with Tukey's *post hoc* test as indicated in the figure legends. $p < 0.05$ was considered to have statistical significance.

Results

AQP4 deficiency eliminates timeliness of voluntary exercise improving cognitive functions of APP/PS1 mice

We assessed the spatial learning and memory of mice using the MWM test. For 5-month-old groups, voluntary exercise intervention reduced the escape latency to find the hidden platform in WT mice ($F_{5,137}$ = 18.72, $p < 0.0001$) and APP/PS1 mice ($F_{5,132}$ = 37.04, $p < 0.0001$), but not AQP4$^{-/-}$/APP/PS1 mice ($F_{5,134}$ = 0.03363, $p = 0.9994$) (Fig. 1b). For 9-month-old groups, exercise shorted the escape latency in WT mice ($F_{5,143}$ = 37.1, $p < 0.0001$), but not APP/PS1 mice ($F_{5,139}$ = 0.2621, $p = 0.933$) or AQP4$^{-/-}$/APP/PS1 mice ($F_{5,136}$ = 0.105, $p = 0.9910$) (Fig. 1c). Time spent in the target quadrant and number of platform crossings during the probe trials on day 7, were high in 5-month-old WT mice and APP/PS1 mice received voluntary exercise ($p = 0.0213$, $p = 0.02$, WT-Exe vs WT-Con; $p = 0.0429$, $p = 0.0442$, APP/PS1-Exe vs APP/PS1-Con, respectively). For 9-month groups, the above parameters were only increased in WT mice with exercise intervention ($p = 0.0126$, $p = 0.027$, respectively). Notably, exercise did not improve spatial memory performance in 5-month-old or 9-month-old AQP4$^{-/-}$/APP/PS1 mice (Fig. 1d-e).

We performed the Y-maze test to measure mouse short-term working memory. For 5-month groups, both WT and APP/PS1 exercise mice exhibited a higher percentage of time spent in the novel arm, when compared with the corresponding sedentary controls ($p = 0.0225$, WT-Exe vs WT-Con; $p = 0.0235$, APP/PS1-Exe vs APP/PS1-Con). Nevertheless the performance of AQP4$^{-/-}$/APP/PS1 mice was comparable between exercise and sedentary groups. For 9-month groups, exercise increased the residence time of WT mice in the novel arm ($p = 0.03$), but failed to reverse working memory deficits in APP/PS1 mice and AQP4$^{-/-}$/APP/PS1 mice (Fig. 1f).

A novel object recognition test was also performed to assess the effect of exercise on recognition memory of mice. For 5-month groups, exercise improved the recognition index of WT mice and APP/PS1 mice ($p = 0.0051$, $p = 0.0392$, respectively), but not AQP4$^{-/-}$/APP/PS1 mice. For 9-month groups, exercise was sufficient to improve recognition memory in WT mice ($p = 0.0467$), but not in APP/PS1 mice and AQP4$^{-/-}$/APP/PS1 mice (Fig. 1g).

AQP4 deficiency in APP/PS1 mice abolishes timeliness of voluntary exercise promoting glymphatic transport

We assessed glymphatic transport by quantifying TR-d3 penetration into the brain parenchyma following injection into the cisterna magna (Fig. 2a). APP/PS1 mice displayed lower of TR-d3 positive area percentage and paravascular fluorescence intensity than WT mice at age of 5 months ($p = 0.0343$, $F_{4,30}$ = 25.09, $p < 0.0001$, respectively) and 9 months ($p = 0.007$, $F_{4,29}$ = 23.7, $p < 0.0001$, respectively). Both 5-month-old and 9-month-old WT mice received voluntary exercise increased fluorescence penetration area ($p = 0.0036$, $p = 0.0067$, respectively) and intensity ($F_{1,28}$ = 39.05, $p < 0.0001$, $F_{1,29}$ = 21.12, $p < 0.0001$, respectively). However, for APP/PS1 mice, the improving effect of exercise on penetration of TR-d3 into the brain parenchyma was observed only in the 5-month group (Area, $p = 0.01$; Intensity, $F_{1,30}$ = 39.27, $p < 0.0001$). Exercise did not increase TR-d3 positive area percentage and paravascular fluorescence

intensity in either 5- or 9-month-old AQP4$^{-/-}$/APP/PS1 mice (Fig. 2b-f). These results suggest that voluntary exercise ameliorates glymphatic transport malfunction in the onset stage rather than mid-stage of APP/PS1 mice, and AQP4 deletion eliminates the promoting effect of exercise on glymphatic transport.

AQP4 deficiency in APP/PS1 mice negates timeliness of voluntary exercise alleviating brain Aβ load

We further evaluated whether the timeliness of voluntary exercise improves glymphatic transport, thereby affecting aggregation of Aβ in the brain of APP/PS1 mice. Compared with age-matched APP/PS1 mice, both 5-month-old and 9-month-old AQP4$^{-/-}$/APP/PS1 mice show more brain Aβ load in the hippocampus and frontal cortex, as revealed quantification of the area percentage and number of thioflavine-S positive fibrillary plaques and 6E10-immunopositive diffuse plaques (all $p < 0.05$). Exercise decreased Aβ plaque accumulation in the above two brain regions of APP/PS1 mice at 5 months (all $p < 0.05$ for the above indexes). The ameliorating effect of exercise on Aβ load was not observed in AQP4$^{-/-}$/APP/PS1 mice at the two different ages (Fig. 3a-f). Consistently, both Western blot and ELISA analysis revealed that voluntary exercise only decreased $A\beta_{1-40}$ and $A\beta_{1-42}$ levels in the forebrain samples of 5-month-old APP/PS1 mice (all $p < 0.05$) rather than 9-month-old APP/PS1 mice. Voluntary exercise failed to decrease brain $A\beta_{1-40}$ and $A\beta_{1-42}$ levels in either 5-or 9-month-old AQP4$^{-/-}$/APP/PS1 mice (Fig. 3g-i; Fig. S1a-b).

Voluntary exercise ameliorates reactive gliosis and neuroinflammation in the onset stage rather than mid-stage of APP/PS1 mice

In addition to Aβ deposition, reactive gliosis is a characteristic pathologic hallmark of AD [34, 35]. We determined effects of voluntary exercise and AQP4 deletion on activation of astrocytes and microglia in APP/PS1 mice at different stages of AD-like progression. Both GFAP-positive astrocytes and Ibal-positive microglia were activated in the frontal cortex and hippocampus of 5-month-old APP/PS1 mice and further apparent in 9 months old. AQP4 deletion in 5-month-old APP/PS1 mice mildly increased activation of microglia and astrocytes in the frontal cortex and hippocampus (Fig. 4a; Fig. 5a; Fig. S2a). Microglia activation was also more pronounced in AQP4$^{-/-}$/APP/PS1 mice at aged 9 months, revealed by high percentages of Iba1 positive area in the frontal cortex ($p = 0.0107$) and hippocampus ($p = 0.0168$) as compared with age-matched APP/PS1 mice. However, a considerable proportion of astrocytes underwent atrophy in 9-month-old AQP4$^{-/-}$/APP/PS1 mice, causing no significant difference in the percentage of GFAP positive area between the two AD mouse lines (Fig. 4a-c, Fig. S2a-d). There was no overall change in immunocytochemical labeling patterns of GFAP and Ibal in the frontal cortex and hippocampus in 5- and 9-month-old WT-exercise mice when compared with age-matched sedentary controls. But it is worth noting that, there were GFAP strong positive glia limitans abutting the pia maters of WT-exercise mice (Fig. 4a and Fig. S2a). As for APP/PS1 mice, exercise reduced the percentages of positive area for GFAP (Cortex, $p = 0.0128$; Hippocampus, $p = 0.0331$) and Iba1 (Cortex, $p = 0.0215$; Hippocampus, $p = 0.0107$) in the 5-month-old group, but not 9-month-old group. Exercise did not mitigate reactivation of astrocytes and microglia in AQP4$^{-/-}$/APP/PS1 mice in the both age groups (Fig. 4a-c and Fig. S2a-d). Consistently, voluntary exercise partially reduced neuroinflammatory factor levels in APP/PS1

mice in 5 months old (IL-1β, $p = 0.0343$; IL-6, $p = 0.045$; TNF-α, $p = 0.031$), but not 9 months old. The Aqp4 knock-out in APP/PS1 mice totally abolished the time-effect of aerobic exercise on neuroinflammation (Fig. 4d).

Voluntary exercise ameliorates impaired polarity of AQP4 in the onset stage rather than mid-stage of APP/PS1 mice

Substantial evidence suggests that reactive astrogliosis results in mislocalization of AQP4 from the endfeet to the entire cell surface of astrocytes, subsequently contributes to glymphatic clearance dysfunction [26, 27, 36]. Both immunofluorescence and immunohistochemical staining revealed that AQP4 expression was selectively bordering the subarachnoid space and microvessels with very low intensity in the adjacent brain parenchyma in WT mice (Fig. 5a, Fig. S3a). AQP4 was abnormally expressed at the non-vascular domains, especially surrounding Aβ plaques, in 5-month-old APP/PS1 mice. The mislocalization of AQP4 was further obvious in the brain parenchyma of 9-month-old APP/PS1 mice, causing total loss of polarity distribution of AQP4. Voluntary exercise reduced astrocyte activation in 5-month-old APP/PS1 mice, in turn improving AQP4 polarity abutting pia mater (Immunofluorescence, $p = 0.005$; Immunohistochemistry, $p = 0.0148$) and microvessels (Immunofluorescence, $p = 0.0302$; Immunohistochemistry, $p = 0.0398$). By contrast, in 9-month-old APP/PS1-exercise mice, this improvement was not apparent because reactive astrogliosis was not reduced (Fig. 5a-c; Fig. S2a-d). WT exercise mice showed increases in AQP4 polarization abutting pia maters (Immunofluorescence: 5-month, $p = 0.0032$, 9-month, $p < 0.0001$, respectively) and microvessels (Immunofluorescence: 5-month, $p = 0.0161$, 9-month, $p = 0.0002$; respectively) (Fig. 5a, Fig. S3a).

AQP4 deficiency eliminates timeliness of voluntary exercise activating BDNF signaling pathway and improving synaptic protein levels in APP/PS1 mice

BDNF signaling pathway is associated with synaptic function and regulates the expression of synaptic proteins such as presynaptic protein SYN and postsynaptic protein PSD-95 [37, 38]. Down regulation of BDNF signaling pathway and synaptic protein loss occur in AD patients [39, 40] as well as animal models of AD [41, 42]. Moreover, BDNF signaling pathway is involved in neuroproection of physical exercise in AD [43, 44], stroke [45, 46] and depression [47, 48]. In this way, the present study measured the activation of BDNF-TrkB-CREB pathway and expression levels of SYN and PSD-95 in the forebrain. The expression levels of mature BDNF, TrkB and p-CREB generally decreased in APP/PS1 mice compared to WT controls aged at 5 months ($p < 0.0001$, $p = 0.005$, $p = 0.009$, respectively) and 9 months ($p = 0.004$, $p = 0.08043$, $p = 0.0174$, respectively). Voluntary activated this signaling pathway in WT mice aged at 5 months (BDNF: $p = 0.0352$, TrkB: $p = 0.0997$, p-CREB: $p = 0.0029$, respectively) and 9 months (BDNF: $p = 0.012$, TrkB: $p = 0.0308$, p-CREB: $p = 0.0402$, respectively), but only in 5-month-old APP/PS1 mice (BDNF: $p = 0.0153$, TrkB: $p = 0.018$, p-CREB: $p = 0.0379$, respectively) (Fig. 6a-b). Consistently, voluntary exercise significantly upregulated SYN and PSD-95 levels in the hippocampus of 5-month-old WT and APP/PS1 mice (all $p < 0.05$), but not $AQP4^{-/-}$/APP/PS1 mice, as revealed by immunohistochemical staining and Western blot analysis (Fig. 6c-d, Fig. S4a-b). For 9-month-old groups, an improving effect of voluntary exercise on the

synaptic protein levels was only observed in WT mice (Immunohistochemistry SYN: $p = 0.0231$, PSD-95: $p = 0.0121$; Western blot: SYN: $p = 0.0113$, PSD-95: $p = 0.0108$).

Discussion

At present, there is a lack of effective pharmacological treatments and other methods for AD. Exploring ways of preventing, or delaying the onset this disease is a pragmatic strategy. Regular exercise can reduce the occurrence of AD in the healthy elderly population and delay the progression of MCI, although the beneficial effect is not apparent in the clinical treatment of AD [6–11]. The underlying mechanism has not yet to be determined. The current study was designed to address this issue. The results show that the beneficial effect of voluntary exercise intervention on AD-like pathology of APP/PS1 mice is time-dependent. Early exercise intervention improves AQP4 polarity, subsequently promoting glymphatic transport while reducing brain Aβ load. However, during the mid-stage of AD-like pathology, AQP4 polarity is disrupted due to reactive astrogliosis. Therefore, exercise intervention is unable to improve glymphatic transport, and has no improving effect on Aβ clearance. Voluntary exercise does not mitigate Aβ accumulation and cognitive impairment of $AQP4^{-/-}$/APP/PS1 mice, further suggesting that AQP4-dependent glymphatic clearance is a key factor for exercise therapy to delay the onset of AD.

Increasing evidence supports the idea that the glymphatic system plays a central role in the clearance of macromolecular substances from the brain [22, 23]. This model of glymphatic system has opened up new perspectives in understanding the pathogenesis of AD [49, 50], stroke [51, 52], brain injury [53] and other neurological diseases [54, 55]. Glymphatic system visualization is not only implemented in animal studies [56, 57], but also being used for clinical imaging diagnosis of hydrocephalus [58, 59] and AD [60]. It is suggested that the driving force of glymphatic transport comes from arterial pulsation, and is facilitated by AQP4 mediated bulk fluid flow from the para-arterial space entering the interstitial space, and finally into the para-venous space [23]. AQP4 gene knockout significantly delays clearance of exogenous Aβ from the brain following intrastriatal injection [23]. Our present and previous studies consistently demonstrate that AQP4 deletion in APP/PS1 mice exacerbates glymphatic clearance impairment and Aβ plaque load [28, 31]. Together, these results indicate that AQP4 is vital for glymphatic clearance, thus playing a critical role in regulating the pathological progress of AD.

The current results further suggest that glymphatic clearance not only depends on the presence of AQP4, but also on its specific localization at the perivascular endfeet of astrocytes. Early studies have shown that glymphatic clearance of exogenous Aβ in aged mice is significantly less than that of young mice [28]. The primary cause is activated astrocytes abnormally expressing AQP4 in the non-perivascular membrane. Aged mice taking part in voluntary exercise exhibit decreased astrocyte activation, improvement of AQP4 polarity, and low brain Aβ concentration, compared to sedentary controls. Consistently, the present results have confirmed that in the onset stage of APP/PS1 mice, voluntary exercise intervention attenuates reactive astrogliosis and mislocalization of AQP4 in the nonvascular domains of the brain parenchyma of astrocytes, subsequently reducing Aβ plaque accumulation. These

results imply that specific expression of AQP4 on the perivascular endfeet of astrocytes is the molecular structural basis for maintaining glymphatic transport.

Additionally, previous studies report that alterations in AQP4 expression and localization in the frontotemporal lobe are associated with AD status and pathology, which is related to noncoding *aqp4* single-nucleotide polymorphisms [61, 62]. Notably, perivascular AQP4 localization is preserved among individuals older than 85 years who remains cognitively intact. Lymphatic transport ability of AD patients has been found to be lower than that of healthy controls of the same age, via assessment of perivascular fluid movement with diffusion tensor MRI [60]. Our recent studies reported that a moderate-intensity aerobic dance improves cognitive function, especially episodic memory and processing speed, in MCI patients [63]. The future studies are necessary for determining whether this protective effect is linked to improving glymphatic transport capacity.

Consistent with the present findings, previous studies report an age-dependent beneficial effect of a continuous non-shock treadmill exercise paradigm on the pathogenic characteristics of APP/PS1 transgenic mice. Five-week of exercise reduces $A\beta_{1-40}$ and $A\beta_{1-42}$ levels in the hippocampus of adult (7–8 month-old) APP/PS1 mice but not aged (24-month-old) APP/PS1 mice, and does not reduce plaque loading in either adult or aged APP/PS1 mice [21]. By contrast, a 4-month treadmill exercise intervention significantly improves spatial learning and memory ability, reduces amyloid plaques in the hippocampus, and induces neurogenesis in the dentate gyrus of 12-month-old APP/PS1 mice [64]. This indicates that a longer exercise intervention may have a more positive effect in delaying the pathological process of AD mice. In addition, exercise of different intensity may bring different effects on APP/PS1 mice. Moderate exercise intensity (60–70% of max oxygen uptake) seems to be more effective in increasing lipid metabolism and reducing soluble Aβ levels, compared with low-intensity exercise (45–55% of maximal oxygen uptake) [65]. Based on this, future studies are also needed to clarify the effects of exercise intensity and duration on glymphatic clearance.

In conclusion, this study has revealed that voluntary exercise promotes the removal of Aβ by the glymphatic system, attenuating its aggregation, and subsequently reducing astrocyte activation, which is conducive to maintain AQP4 polarity. This effect, in turn, maintains glymphatic transport capability, thereby effectively promoting cognitive function of adult WT mice and delaying the onset of AD-like pathogenesis in APP/PS1 mice. Long-term voluntary exercise intervention fails to improve Aβ clearance and alleviate AD-like pathology under AQP4 deficiency or AQP4 polarity damage condition. These results highlight that AQP4-dependent glymphatic transport is the neural basis for exercise against AD. The finding has revealed the molecular pathology mechanism that exercise helps prevent AD, but cannot treat AD, which is a long-standing dilemma in the field of AD research. Keeping a certain amount of exercise vitality is a convenient, effective and simple way to prevent the onset of AD.

Abbreviations

AD: Alzheimer's disease; ANOVA: Analysis of variance; AQP4: aquaporin-4; BDNF: brain-derived neurotrophic factor; CREB: cyclic adenosine monophosphate response element binding protein; GAPDH: glyceraldehyde-3-phosphate dehydrogenase; GFAP: glial fibrillary acid protein; Iba-1: ionized calcium binding adaptor molecule 1; IL-1β: interleukin 1β; IL-6: interleukin 6; MWM: Morris water maze; NORT: novel object recognition test; PSD-95: postsynaptic density protein 95; SYN: synaptophysin; TrkB: tropomyosin receptor kinase B; TNF-α: tumor necrosis factor-α; TR-d3: Texas Red-dextran-3; WT: Wild-type.

Declarations

Ethics approval and consent to participate

All procedures were approved by Institutional Animal Care and Use Committee of Nanjing Medical University (IACUC-1601106).

Consent for publication

Not applicable.

Availability of data and material

All data mentioned in this article are available on published article.

Competing interests

Authors have no conflict of interest to declare.

Funding

This study was supported by grants from the National Natural Science Foundation of China (No. 81772454 and No. 81671070).

Authors' contributions

YL, XW, RZ, PH and SZ performed experiments and statistical analyses. YL, XW and QL were involved in interpretation of data. TW made substantial contributions to design experiment. YL and MX wrote the manuscript. CM revised the article for important intellectual content. All authors read and approved the final version of the article.

Acknowledgments

Not applicable.

References

1. Querfurth HW, LaFerla FM. Alzheimer's disease. N Engl J Med. 2010;362(4):329-44.
2. Caselli RJ, Beach TG, Knopman DS, Graff-Radford NR. Alzheimer Disease: Scientific Breakthroughs and Translational Challenges. Mayo Clin Proc. 2017;92(6):978-94.
3. Kivipelto M, Mangialasche F, Ngandu T. Lifestyle interventions to prevent cognitive impairment, dementia and Alzheimer disease. Nat Rev Neurol. 2018;14(11):653-66.
4. Larson EB, Wang L, Bowen JD, McCormick WC, Teri L, Crane P, Kukull W. Exercise is associated with reduced risk for incident dementia among persons 65 years of age and older. Ann Intern Med. 2006;144(2):73-81.
5. Richards M, Hardy R, Wadsworth ME. Does active leisure protect cognition? Evidence from a national birth cohort. Soc Sci Med. 2003;56(4):785-92.
6. Zhang Y, Li C, Zou L, Liu X, Song W. The effects of mind-body exercise on cognitive performance in elderly: A systematic review and meta-analysis. Int J Environ Res Public Health. 2018;15(12):2791.
7. Law LL, Barnett F, Yau MK, Gray MA. Effects of functional tasks exercise on older adults with cognitive impairment at risk of Alzheimer's disease: a randomised controlled trial. Age Ageing. 2014;43(6):813-20.
8. Law CK, Lam FM, Chung RC, Pang MY. Physical exercise attenuates cognitive decline and reduces behavioural problems in people with mild cognitive impairment and dementia: a systematic review. J Physiother. 2020;66(1):9-18.
9. Blondell SJ, Hammersley-Mather R, Veerman JL. Does physical activity prevent cognitive decline and dementia?: A systematic review and meta-analysis of longitudinal studies. BMC Public Health. 2014;14:510.
10. de Oliveira Silva F, Ferreira JV, Plácido J, Sant'Anna P, Araújo J, Marinho V, Laks J, Camaz Deslandes A. Three months of multimodal training contributes to mobility and executive function in elderly individuals with mild cognitive impairment, but not in those with Alzheimer's disease: A randomized controlled trial. Maturitas. 2019;126:28-33.
11. Forbes D, Forbes SC, Blake CM, Thiessen EJ, Forbes S. Exercise programs for people with dementia. Cochrane Database Syst Rev. 2015;(4):CD006489.
12. Jahangiri Z, Gholamnezhad Z, Hosseini M. Neuroprotective effects of exercise in rodent models of memory deficit and Alzheimer's. Metab Brain Dis. 2019;34(1):21-37.
13. Quan H, Koltai E, Suzuki K, Aguiar Júnior AS, Pinho R, Boldogh I, Berkes I, Radak Z. Exercise, redox system and neurodegenerative diseases. Biochim Biophys Acta Mol Basis Dis. 2020:165778.
14. Adlard PA, Perreau VM, Pop V, Cotman CW. Voluntary exercise decreases amyloid load in a transgenic model of Alzheimer's disease. J Neurosci. 2005;25(17):4217-21.
15. Xia J, Li B, Yin L, Zhao N, Yan Q, Xu B. Treadmill exercise decreases β-amyloid burden in APP/PS1 transgenic mice involving regulation of the unfolded protein response. Neurosci Lett. 2019;703:125-31.

16. Zhang X, He Q, Huang T, Zhao N, Liang F, Xu B, Chen X, Li T, Bi J. Treadmill exercise decreases Aβ deposition and counteracts cognitive decline in APP/PS1 mice, possibly via hippocampal microglia modifications. Front Aging Neurosci. 2019;11:78.
17. Francis N, Robison LS, Popescu DL, Michaelos M, Hatfield J, Xu F, Zhu X, Davis J, Anderson ME, Anderson BJ, Van Nostrand WE, Robinson JK. Voluntary wheel running reduces amyloid-β42 and rescues behavior in aged Tg2576 mouse model of Alzheimer's disease. J Alzheimers Dis. 2020;73(1):359-74.
18. Wolf SA, Kronenberg G, Lehmann K, Blankenship A, Overall R, Staufenbiel M, Kempermann G. Cognitive and physical activity differently modulate disease progression in the amyloid precursor protein (APP)-23 model of Alzheimer's disease. Biol Psychiatry. 2006;60(12):1314-23.
19. Robison LS, Popescu DL, Anderson ME, Francis N, Hatfield J, Sullivan JK, Beigelman SI, Xu F, Anderson BJ, Van Nostrand WE, Robinson JK. Long-term voluntary wheel running does not alter vascular amyloid burden but reduces neuroinflammation in the Tg-SwDI mouse model of cerebral amyloid angiopathy. J Neuroinflammation. 2019;16(1):144.
20. Xu ZQ, Zhang LQ, Wang Q, et al. Aerobic exercise combined with antioxidative treatment does not counteract moderate-or mid-stage Alzheimer-like pathophysiology of APP/PS1 mice. CNS Neurosci Ther. 2013;19(10):795-803.
21. Ke HC, Huang HJ, Liang KC, Hsieh-Li HM. Selective improvement of cognitive function in adult and aged APP/PS1 transgenic mice by continuous non-shock treadmill exercise. Brain Res. 2011;1403:1-11.
22. Xin SH, Tan L, Cao X, Yu JT, Tan L. Clearance of amyloid beta and Tau in Alzheimer's disease: from mechanisms to therapy. Neurotox Res. 2018;34(3):733-48.
23. Iliff JJ, Wang M, Liao Y, Plogg BA, Peng W, Gundersen GA, Benveniste H, Vates GE, Deane R, Goldman SA, Nagelhus EA, Nedergaard M. A paravascular pathway facilitates CSF flow through the brain parenchyma and the clearance of interstitial solutes, including amyloid β. Sci Transl Med. 2012;4(147):147ra111.
24. Mestre H, Hablitz LM, Xavier AL, Feng W, Zou W, Pu T, Monai H, Murlidharan G, Castellanos Rivera RM, Simon MJ, Pike MM, Plá V, Du T, Kress BT, Wang X, Plog BA, Thrane AS, Lundgaard I, Abe Y, Yasui M, Thomas JH, Xiao M, Hirase H, Asokan A, Iliff JJ, Nedergaard M. Aquaporin-4-dependent glymphatic solute transport in the rodent brain. Elife. 2018;7:e40070.
25. Nedergaard M, Goldman SA. Brain drain. Sci Am. 2016; 314(3): 44-9.
26. Kress BT, Iliff JJ, Xia M, Wang M, Wei HS, Zeppenfeld D, Xie L, Kang H, Xu Q, Liew JA, Plog BA, Ding F, Deane R, Nedergaard M. Impairment of paravascular clearance pathways in the aging brain. Ann Neurol. 2014;76(6):845-61.
27. Wang L, Zhang Y, Zhao Y, Marshall C, Wu T, Xiao M. Deep cervical lymph node ligation aggravates AD-like pathology of APP/PS1 mice. Brain Pathol. 2019;29(2):176-92.
28. Xu Z, Xiao N, Chen Y, Huang H, Marshall C, Gao J, Cai Z, Wu T, Hu G, Xiao M. Deletion of aquaporin-4 in APP/PS1 mice exacerbates brain Aβ accumulation and memory deficits. Mol Neurodegener.

2015;10(1):58.

29. He XF, Liu DX, Zhang Q, Liang FY, Dai GY, Zeng JS, Pei Z, Xu GQ, Lan Y. Voluntary exercise promotes glymphatic clearance of amyloid beta and reduces the activation of astrocytes and microglia in aged Mice. Front Mol Neurosci. 2017;10:144.
30. Trinchese F, Liu S, Battaglia F, Walter S, Mathews PM, Arancio O. Progressive age-related development of Alzheimer-like pathology in APP/PS1 mice. Ann Neurol. 2004;55:801-14.
31. Feng W, Zhang Y, WangZ, Xu H, Wu T, Marshall C, Gao J, Xiao M. Microglia prevent beta-amyloid plaque formation in the early stage of an Alzheimer's disease mouse model with suppression of glymphatic clearance. Alzheimers Res Ther. 2020;12(1):125.
32. Peng W, Achariyar TM, Li B, Liao Y, Mestre H, Hitomi E, Regan S, Kasper T, Peng S, Ding F, Benveniste H, Nedergaard M, Deane R. Suppression of glymphatic fluid transport in a mouse model of Alzheimer's disease. Neurobiol Dis. 2016;93:215-25.
33. Lueptow LM. Novel object recognition test for the investigation of learning and memory in mice. J Vis Exp. 2017;126:55718.
34. Acosta C, Anderson HD, Anderson CM. Astrocyte dysfunction in Alzheimer disease. J Neurosci Res. 2017;95(12):2430-47.
35. Lopategui Cabezas I, Herrera Batista A, Pentón Rol G. The role of glial cells in Alzheimer disease: potential therapeutic implications. Neurologia. 2014;29(5):305-9.
36. Iliff JJ, Chen MJ, Plog BA, Zeppenfeld DM, Soltero M, Yang L, Singh I, Deane R, Nedergaard M. Impairment of glymphatic pathway function promotes tau pathology after traumatic brain injury. J Neurosci. 2014;34(49):16180-93.
37. Chao, M. Neurotrophins and their receptors: A convergence point for many signalling pathways. Nat Rev Neurosci. 2003;4(4):299-309.
38. Poo MM. Neurotrophins as synaptic modulators. Nat Rev Neurosci. 2001;2(1):24-32.
39. Peng S, Wuu J, Mufson EJ, Fahnestock M. Precursor form of brain-derived neurotrophic factor and mature brain-derived neurotrophic factor are decreased in the pre-clinical stages of Alzheimer's disease. J Neurochem. 2005;93(6):1412-21.
40. Kim BY, Lee SH, Graham PL, Angelucci F, Lucia A, Pareja-Galeano H, Leyhe T, Turana Y, Lee IR, Yoon JH, Shin JI. Peripheral brain-derived neurotrophic factor levels in Alzheimer's disease and mild cognitive impairment: a comprehensive systematic review and meta-analysis. Mol Neurobiol. 2017;54(9):7297-311.
41. Bartolotti N, Segura L, Lazarov O. Diminished CRE-induced plasticity is linked to memory deficits in familial Alzheimer's disease mice. J Alzheimers Dis. 2016;50(2):477-89.
42. Poon WW, Blurton-Jones M, Tu CH, Feinberg LM, Chabrier MA, Harris JW, Jeon NL, Cotman CW. β-Amyloid impairs axonal BDNF retrograde trafficking. Neurobiol Aging. 2011;32(5):821-33.
43. Vaynman S, Ying Z, Gómez-Pinilla F. Exercise induces BDNF and synapsin I to specific hippocampal subfields. J Neurosci Res. 2004;76(3):356-62.

44. Liu PZ, Nusslock R. Exercise-mediated neurogenesis in the hippocampus via BDNF. Front Neurosci. 2018;12:52.
45. Liu W, Wang X, O'Connor M, Wang G, Han F. Brain-derived neurotrophic factor and its potential therapeutic role in stroke comorbidities. Neural Plast. 2020;2020:1969482.
46. Ferrer I, Krupinski J, Goutan E, Martí E, Ambrosio S, Arenas E. Brain-derived neurotrophic factor reduces cortical cell death by ischemia after middle cerebral artery occlusion in the rat. Acta Neuropathol. 2001;101(3):229-38.
47. Duman RS, Monteggia LM. A neurotrophic model for stress-related mood disorders. Biol Psychiatry. 2006;59(12):1116-27.
48. Martinowich K, Manji H, Lu B. New insights into BDNF function in depression and anxiety. Nat Neurosci. 2007;10(9):1089-93.
49. Reeves BC, Karimy JK, Kundishora AJ, Mestre H, Cerci HM, Matouk C, Alper SL, Lundgaard I, Nedergaard M, Kahle KT. Glymphatic system impairment in Alzheimer's disease and idiopathic normal pressure hydrocephalus. Trends Mol Med. 2020;26(3):285-95.
50. Valenza M, Facchinetti R, Steardo L, Scuderi C. Altered waste disposal system in aging and Alzheimer's disease: Focus on astrocytic aquaporin-4. Front Pharmacol. 2020;10:1656.
51. Mestre H, Du T, Sweeney AM, Liu G, Samson AJ, Peng W, Mortensen KN, Stæger FF, Bork PAR, Bashford L, Toro ER, Tithof J, Kelley DH, Thomas JH, Hjorth PG, Martens EA, Mehta RI, Solis O, Blinder P, Kleinfeld D, Hirase H, Mori Y, Nedergaard M. Cerebrospinal fluid influx drives acute ischemic tissue swelling. Science. 2020;367(6483):eaax7171.
52. Goulay R, Mena Romo L, Hol EM, Dijkhuizen RM. From stroke to dementia: a comprehensive review exposing tight interactions between stroke and amyloid-β formation. Transl Stroke Res. 2020;11(4):601-14.
53. Piantino J, Lim MM, Newgard CD, Iliff J. Linking traumatic brain injury, sleep disruption and post-traumatic headache: a potential role for glymphatic pathway dysfunction. Curr Pain Headache Rep. 2019;23(9):62.
54. Nikolenko VN, Oganesyan MV, Vovkogon AD, Nikitina AT, Sozonova EA, Kudryashova VA, Rizaeva NA, Cabezas R, Avila-Rodriguez M, Neganova ME, Mikhaleva LM, Bachurin SO, Somasundaram SG, Kirkland CE, Tarasov VV, Aliev G. Current understanding of central nervous system drainage systems: implications in the context of neurodegenerative diseases. Curr Neuropharmacol. 2019. doi: 10.2174/1570159X17666191113103850. [Epub ahead of print]
55. Rasmussen MK, Mestre H, Nedergaard M. The glymphatic pathway in neurological disorders. Lancet Neurol. 2018;17(11):1016-24.
56. Harrison IF, Siow B, Akilo AB, Evans PG, Ismail O, Ohene Y, Nahavandi P, Thomas DL, Lythgoe MF, Wells JA. Non-invasive imaging of CSF-mediated brain clearance pathways via assessment of perivascular fluid movement with diffusion tensor MRI. Elife. 2018;7:e34028.
57. Komlosh ME, Benjamini D, Williamson NW, Horkay F, Hutchinson EB, Basser PJ. A novel MRI phantom to study interstitial fluid transport in the glymphatic system. Magn Reson Imaging.

2019;56:181-6.
58. Ringstad G, Vatnehol SAS, Eide PK. Glymphatic MRI in idiopathic normal pressure hydrocephalus. Brain. 2017;140(10):2691-705.
59. Yokota H, Vijayasarathi A, Cekic M, Hirata Y, Linetsky M, Ho M, Kim W, Salamon N. Diagnostic performance of glymphatic system evaluation using diffusion tensor imaging in idiopathic normal pressure hydrocephalus and mmickers. Curr Gerontol Geriatr Res. 2019;2019:5675014.
60. Taoka T, Masutani Y, Kawai H, Nakane T, Matsuoka K, Yasuno F, Kishimoto T, Naganawa S. Evaluation of glymphatic system activity with the diffusion MR technique: diffusion tensor image analysis along the perivascular space (DTI-ALPS) in Alzheimer's disease cases. Jpn J Radiol. 2017;35(4):172-8.
61. Zeppenfeld DM, Simon M, Haswell JD, D'Abreo D, Murchison C, Quinn JF, Grafe MR, Woltjer RL, Kaye J, Iliff JJ. Association of perivascular localization of aquaporin-4 with cognition and Alzheimer disease in aging brains. JAMA Neurol. 2017;74(1):91-9.
62. Burfeind KG, Murchison CF, Westaway SK, Simon MJ, Erten-Lyons D, Kaye JA, Quinn JF, Iliff JJ. The effects of noncoding aquaporin-4 single-nucleotide polymorphisms on cognition and functional progression of Alzheimer's disease. Alzheimers Dement (N Y). 2017;3(3):348-59.
63. Zhu Y, Wu H, Qi M, Wang S, Zhang Q, Zhou L, Wang S, Wang W, Wu T, Xiao M, Yang S, Chen H, Zhang L, Zhang KC, Ma J, Wang T. Effects of a specially designed aerobic dance routine on mild cognitive impairment. Clin Interv Aging. 2018;13:1691-700.
64. Chao F, Jiang L, Zhang Y, Zhou C, Zhang L, Tang J, Liang X, Qi Y, Zhu Y, Ma J, Tang Y. Stereological Investigation of the Effects of Treadmill Running Exercise on the Hippocampal Neurons in Middle-Aged APP/PS1 Transgenic Mice. J Alzheimers Dis. 2018;63(2):689-703.
65. Zeng B, Zhao G, Liu HL. The differential effect of treadmill exercise intensity on hippocampal soluble Aβ and lipid metabolism in APP/PS1 mice. Neuroscience. 2020;430:73-81.

Figures

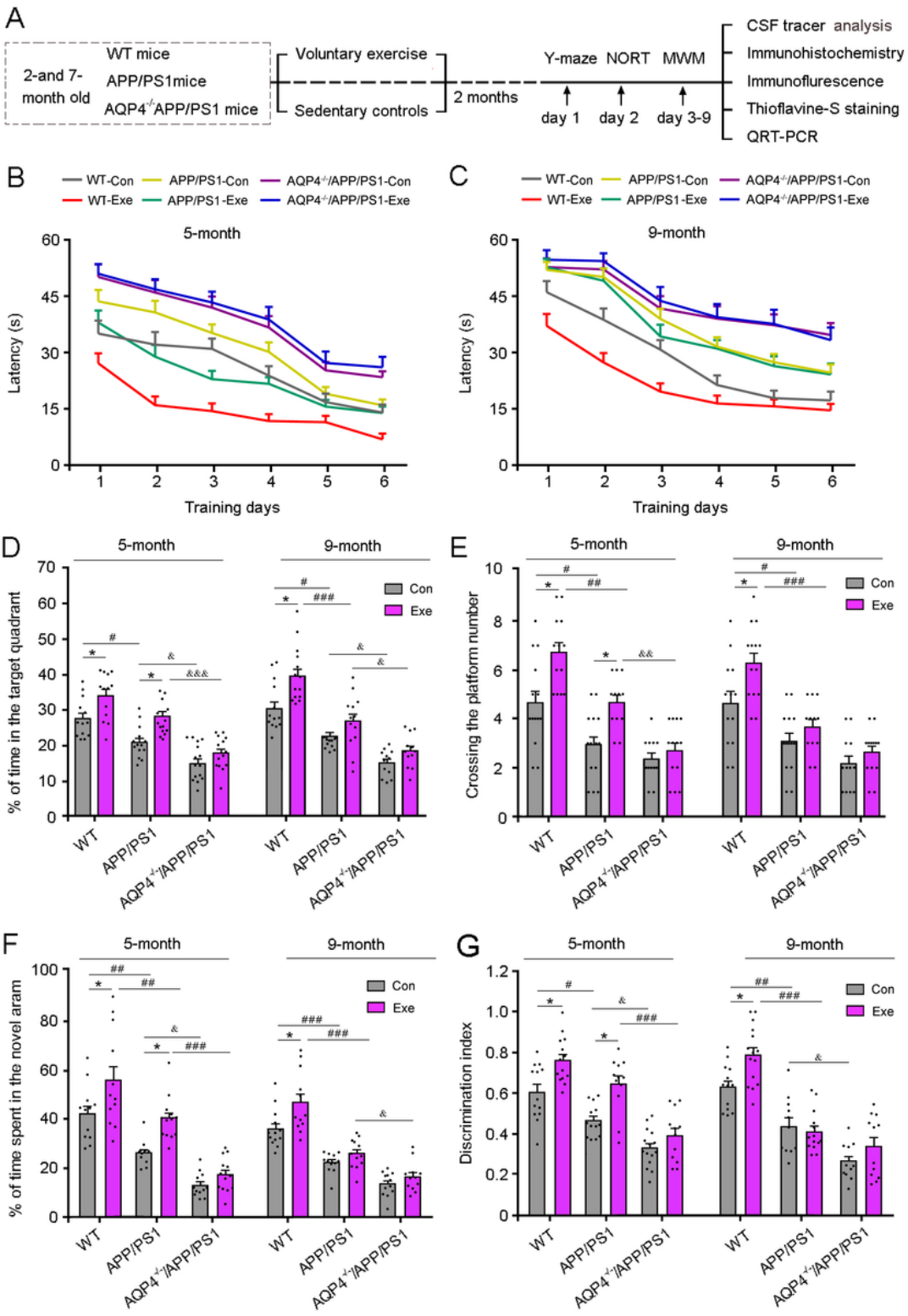

Figure 1

The effect of voluntary exercise on cognitive function in 5- and 9-month-old APP/PS1 mice with or without AQP4. a Schematic representation of the experimental design. Two and several months old WT mice, APP/PS1 mice and AQP4-/-/APP/PS1 mice were randomly assigned to voluntary exercise group or sedentary control group. The mice in each group were given the corresponding treatment for 2 months and then tested by the Y-maze, novel object recognition test (NORT) and Morris water maze (MWM)

followed by pathological and biochemical analyses. b-c The mean escape latency during the hidden platform training period of the MWM of 5-month-old groups (b) and 9-month-old groups (c). d The percentage of time spent in the target quadrant. e The number of crossing the platform area. f The percentage of time spent in the novel arm of Y-maze. g The recognition index in the NORT. Data in b and c were analyzed by the repeated-measures ANOVA with post hoc Student-Newman-Keuls test. Data in d-g were analyzed by the three-way factor ANOVA with Tukey's post hoc test. Data represent mean ± SEM from 12-15 mice per group. *p < 0.05, **p < 0.01, Exercise versus Control; #p < 0.05, ##p < 0.01, ###p < 0.001, APP/PS1 versus WT; &p < 0.05, &&p < 0.01, &&&p < 0.001, AQP4−/−/APP/PS1 versus APP/PS1.

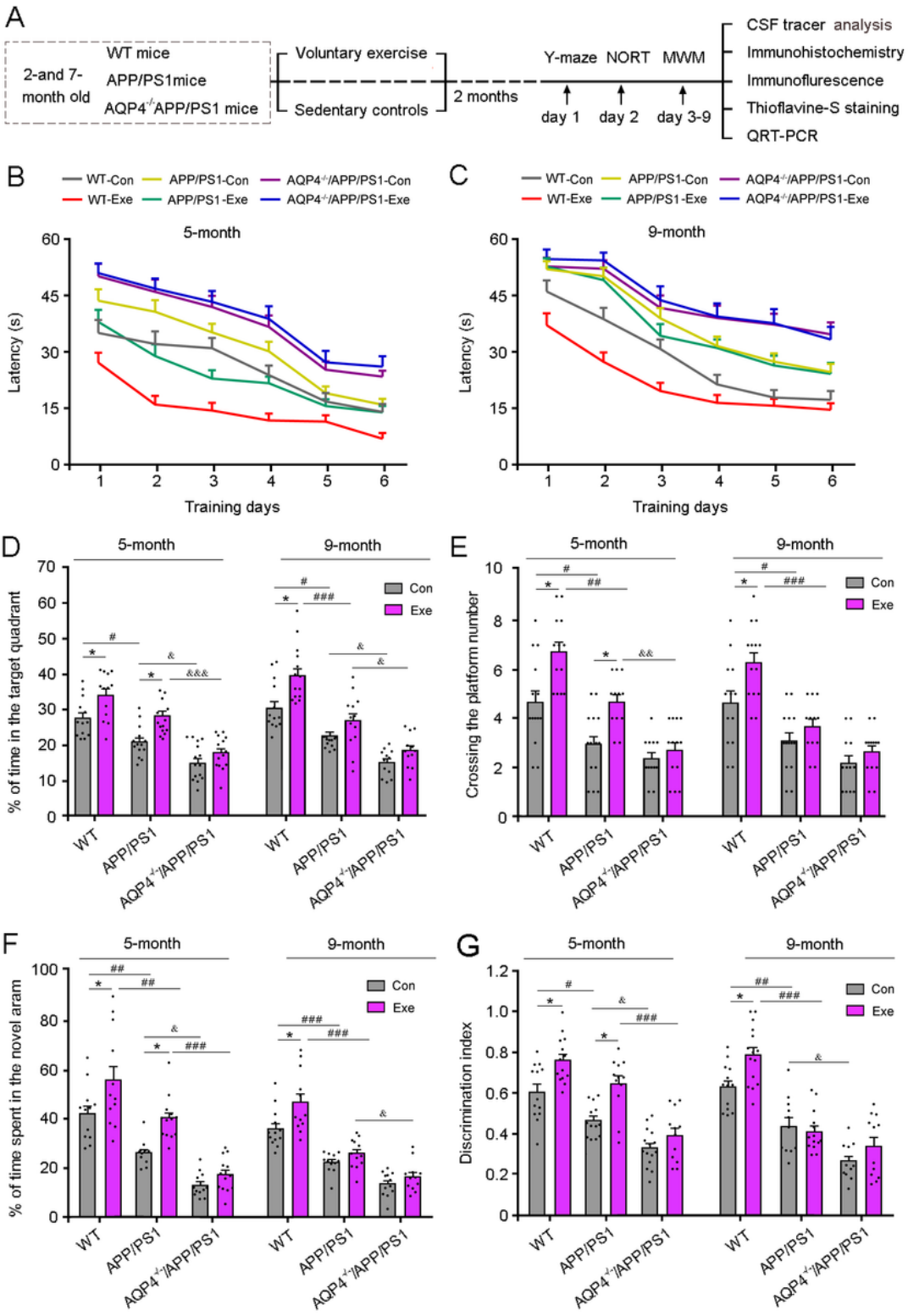

Figure 1

The effect of voluntary exercise on cognitive function in 5- and 9-month-old APP/PS1 mice with or without AQP4. a Schematic representation of the experimental design. Two and several months old WT mice, APP/PS1 mice and AQP4-/-/APP/PS1 mice were randomly assigned to voluntary exercise group or sedentary control group. The mice in each group were given the corresponding treatment for 2 months and then tested by the Y-maze, novel object recognition test (NORT) and Morris water maze (MWM)

followed by pathological and biochemical analyses. b-c The mean escape latency during the hidden platform training period of the MWM of 5-month-old groups (b) and 9-month-old groups (c). d The percentage of time spent in the target quadrant. e The number of crossing the platform area. f The percentage of time spent in the novel arm of Y-maze. g The recognition index in the NORT. Data in b and c were analyzed by the repeated-measures ANOVA with post hoc Student-Newman-Keuls test. Data in d-g were analyzed by the three-way factor ANOVA with Tukey's post hoc test. Data represent mean ± SEM from 12-15 mice per group. *p < 0.05, **p < 0.01, Exercise versus Control; #p < 0.05, ##p < 0.01, ###p < 0.001, APP/PS1 versus WT; &p < 0.05, &&p < 0.01, &&&p < 0.001, AQP4−/−/APP/PS1 versus APP/PS1.

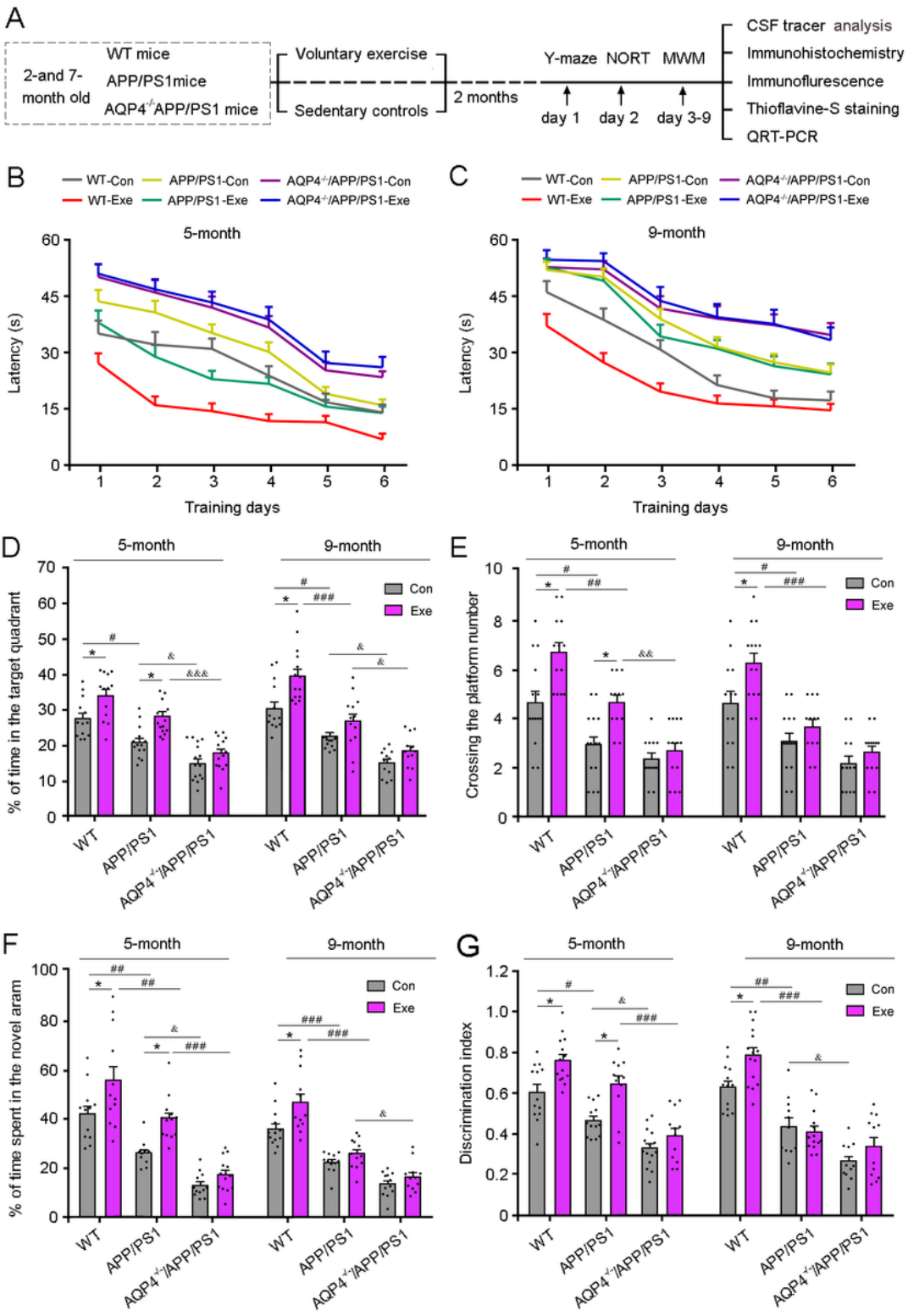

Figure 1

The effect of voluntary exercise on cognitive function in 5- and 9-month-old APP/PS1 mice with or without AQP4. a Schematic representation of the experimental design. Two and several months old WT mice, APP/PS1 mice and AQP4-/-/APP/PS1 mice were randomly assigned to voluntary exercise group or sedentary control group. The mice in each group were given the corresponding treatment for 2 months and then tested by the Y-maze, novel object recognition test (NORT) and Morris water maze (MWM)

followed by pathological and biochemical analyses. b-c The mean escape latency during the hidden platform training period of the MWM of 5-month-old groups (b) and 9-month-old groups (c). d The percentage of time spent in the target quadrant. e The number of crossing the platform area. f The percentage of time spent in the novel arm of Y-maze. g The recognition index in the NORT. Data in b and c were analyzed by the repeated-measures ANOVA with post hoc Student-Newman-Keuls test. Data in d-g were analyzed by the three-way factor ANOVA with Tukey's post hoc test. Data represent mean ± SEM from 12-15 mice per group. *p < 0.05, **p < 0.01, Exercise versus Control; #p < 0.05, ##p < 0.01, ###p < 0.001, APP/PS1 versus WT; &p < 0.05, &&p < 0.01, &&&p < 0.001, AQP4−/−/APP/PS1 versus APP/PS1.

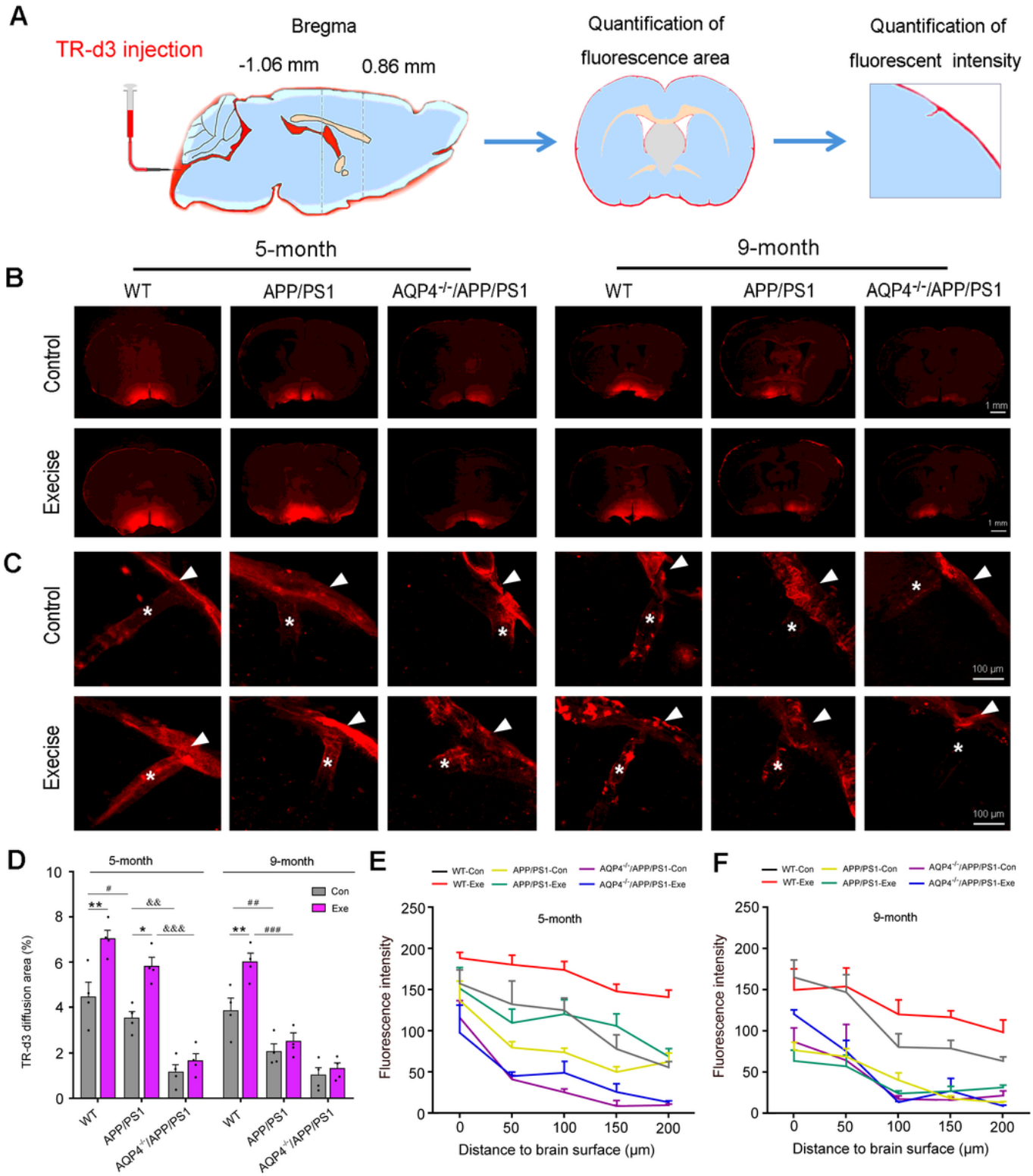

Figure 2

The effect of voluntary exercise on glymphatic transport in 5- and 9-month-old APP/PS1 mice with or without AQP4. a Schematic diagram for intracisternal injection of TR-d3 tracer and experiment schedule. b Representative images of coronal brain sections of each group at bregma 0 mm showing TR-d3 influx into the brain at 40 min after cisterna magna injection. c High magnification micrographs of the frontal cortex showing TR-d3 distribution on the brain surface (arrowheads) and within the perivascular space

(stars). d Quantification of the area percentage of TR-d3 fluorescence in the brain section. e-f Quantification of the mean fluorescence intensity of TR-d3 along the perivascular space. Data in d were analyzed by the three-way factor ANOV with Tukey's post hoc test. Data in e and f were analyzed by the repeated-measures ANOVA with post hoc Student-Newman-Keuls test. Data represent mean ± SEM from 4 sections (in d) or 6-8 microvessels (in e and f) per mouse, and four mice per group. *p < 0.05, **p < 0.01, Exercise versus Control; #p < 0.05, ###p < 0.001, APP/PS1 versus WT; &&p < 0.01, &&&p < 0.001, AQP4−/−/APP/PS1 versus APP/PS1.

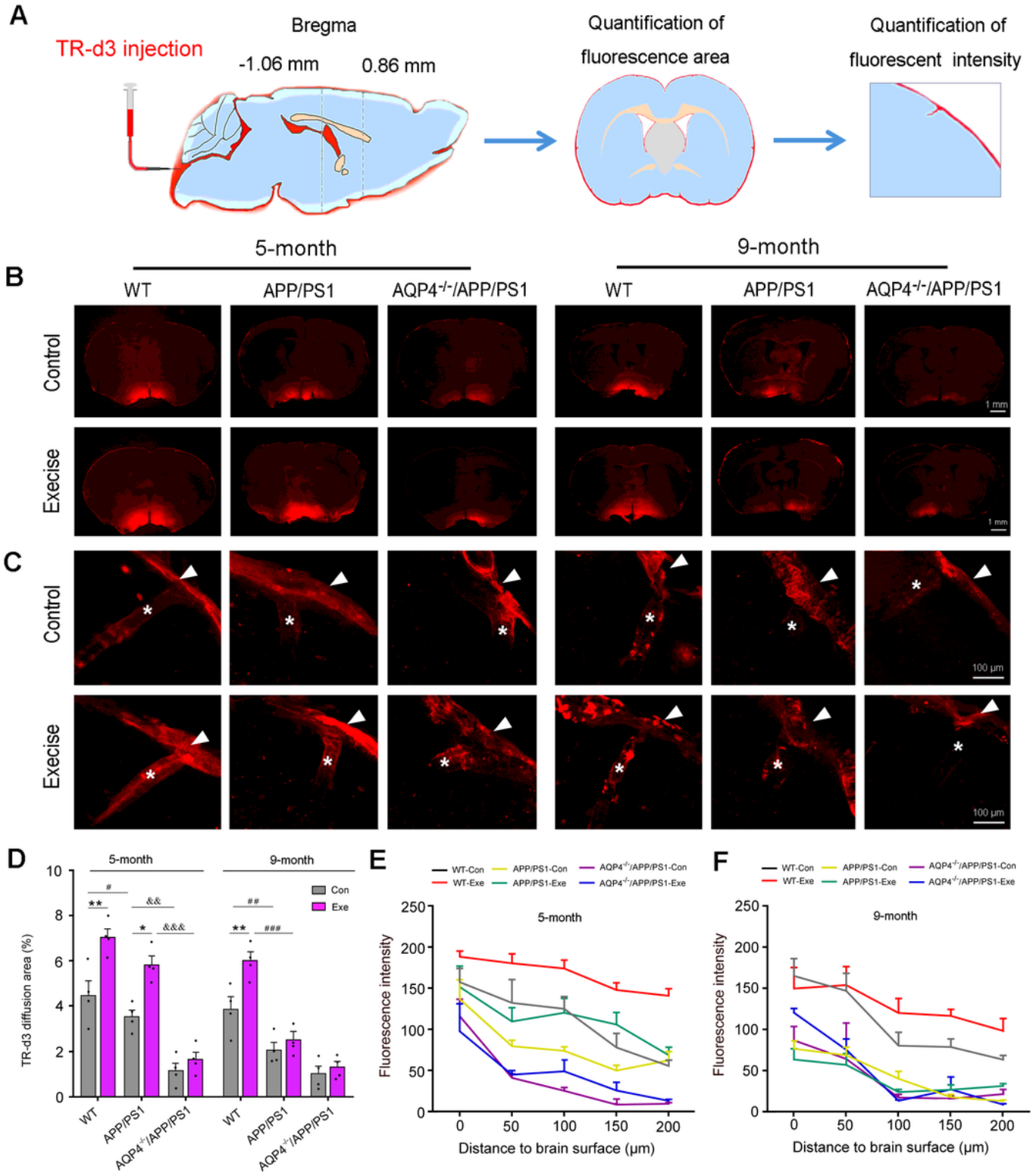

Figure 2

The effect of voluntary exercise on glymphatic transport in 5- and 9-month-old APP/PS1 mice with or without AQP4. a Schematic diagram for intracisternal injection of TR-d3 tracer and experiment schedule. b Representative images of coronal brain sections of each group at bregma 0 mm showing TR-d3 influx into the brain at 40 min after cisterna magna injection. c High magnification micrographs of the frontal cortex showing TR-d3 distribution on the brain surface (arrowheads) and within the perivascular space (stars). d Quantification of the area percentage of TR-d3 fluorescence in the brain section. e-f Quantification of the mean fluorescence intensity of TR-d3 along the perivascular space. Data in d were analyzed by the three-way factor ANOV with Tukey's post hoc test. Data in e and f were analyzed by the repeated-measures ANOVA with post hoc Student-Newman-Keuls test. Data represent mean ± SEM from 4 sections (in d) or 6-8 microvessels (in e and f) per mouse, and four mice per group. *p < 0.05, **p < 0.01, Exercise versus Control; #p < 0.05, ###p < 0.001, APP/PS1 versus WT; &&p < 0.01, &&&p < 0.001, AQP4−/−/APP/PS1 versus APP/PS1.

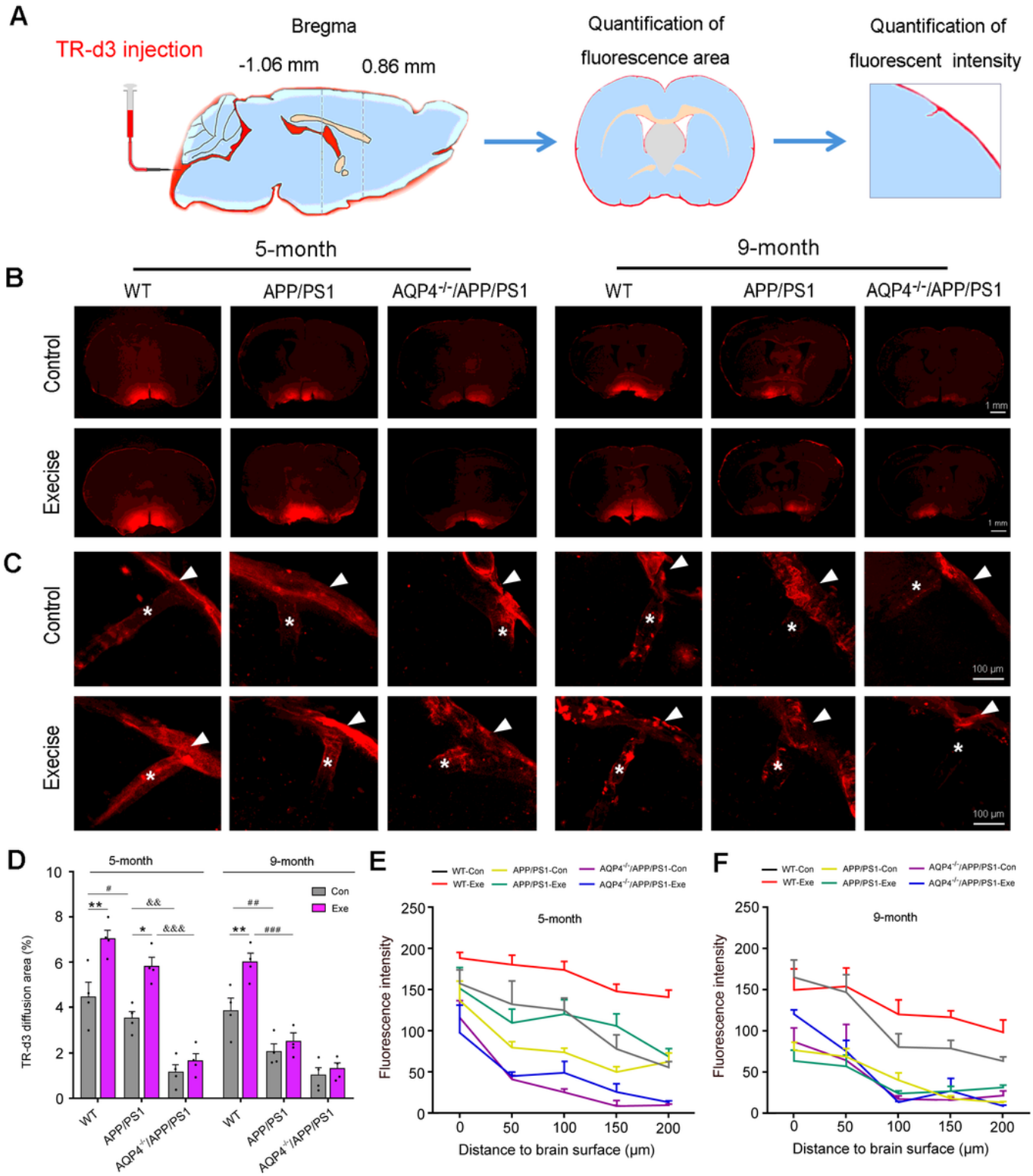

Figure 2

The effect of voluntary exercise on glymphatic transport in 5- and 9-month-old APP/PS1 mice with or without AQP4. a Schematic diagram for intracisternal injection of TR-d3 tracer and experiment schedule. b Representative images of coronal brain sections of each group at bregma 0 mm showing TR-d3 influx into the brain at 40 min after cisterna magna injection. c High magnification micrographs of the frontal cortex showing TR-d3 distribution on the brain surface (arrowheads) and within the perivascular space

(stars). d Quantification of the area percentage of TR-d3 fluorescence in the brain section. e-f Quantification of the mean fluorescence intensity of TR-d3 along the perivascular space. Data in d were analyzed by the three-way factor ANOV with Tukey's post hoc test. Data in e and f were analyzed by the repeated-measures ANOVA with post hoc Student-Newman-Keuls test. Data represent mean ± SEM from 4 sections (in d) or 6-8 microvessels (in e and f) per mouse, and four mice per group. *p < 0.05, **p < 0.01, Exercise versus Control; #p < 0.05, ###p < 0.001, APP/PS1 versus WT; &&p < 0.01, &&&p < 0.001, AQP4−/−/APP/PS1 versus APP/PS1.

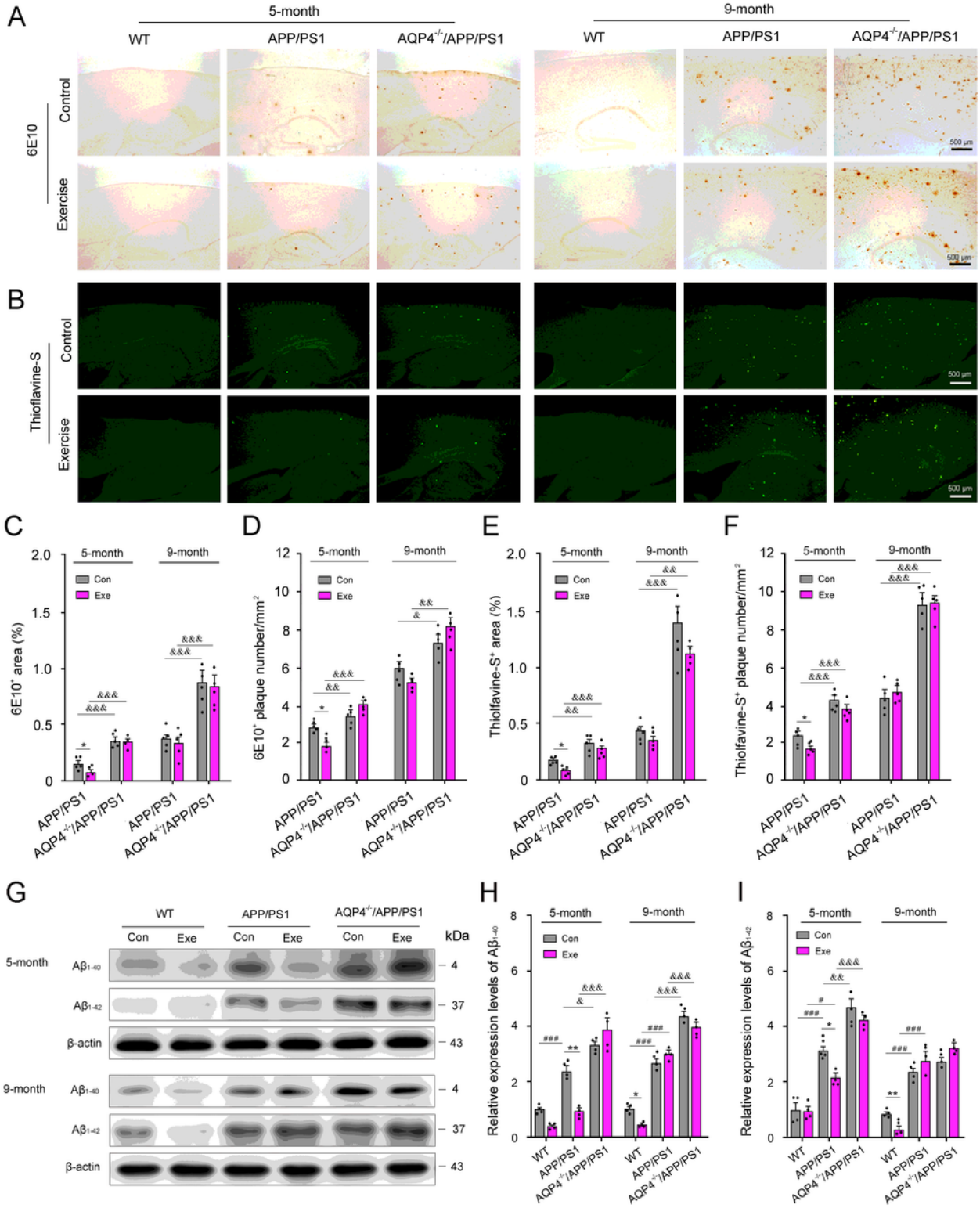

Figure 3

The effect of voluntary exercise on Aβ accumulation in 5- and 9-month-old APP/PS1 mice with or without AQP4. a-b 6E10 immunostaining and thioflavine-S staining showing Aβ plaques in the hippocampus and adjacent cortex, respectively. c-d The area percentage and number of 6E10-immunopositive diffuse plaques. e-f The area percentage and number of thioflavine-S positive fibrillary plaques. g-i Representative bands of Western bolt and densitometry analysis of Aβ1-40 and Aβ1-42 expression levels in the hippocampus. Data are analyzed by the three-way factor ANOVA with Tukey's post hoc test and represent mean ± SEM from 5 sections per mouse (in c-f) or three independent experiments (in h-i) and four mice per group. *p < 0.05, **p < 0.01, Exercise versus Control; #p < 0.05, ###p < 0.001, APP/PS1 versus WT; &p < 0.05, &&p < 0.01, &&&p < 0.001, AQP4−/−/APP/PS1 versus APP/PS1.

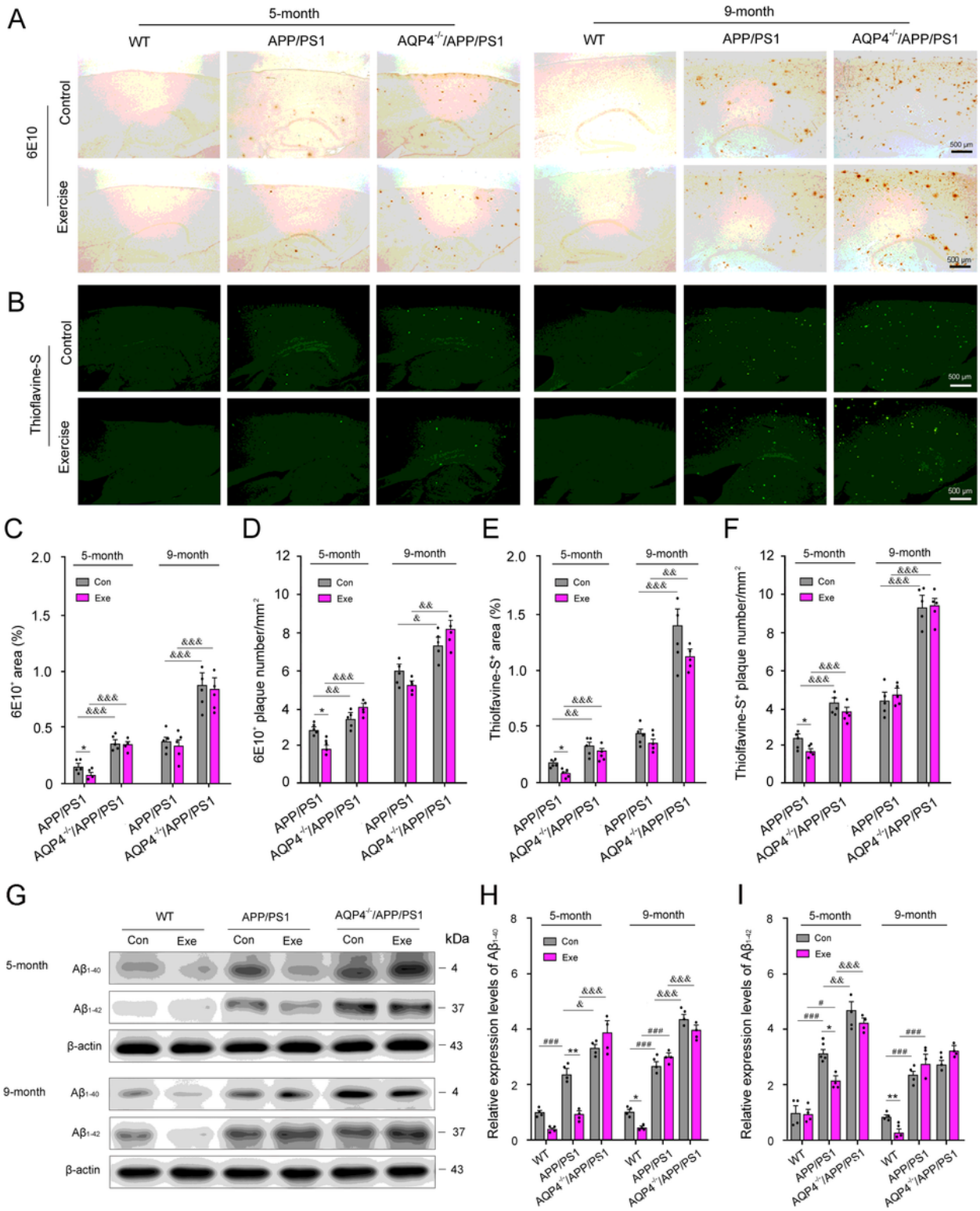

Figure 3

The effect of voluntary exercise on Aβ accumulation in 5- and 9-month-old APP/PS1 mice with or without AQP4. a-b 6E10 immunostaining and thioflavine-S staining showing Aβ plaques in the hippocampus and adjacent cortex, respectively. c-d The area percentage and number of 6E10-immunopositive diffuse plaques. e-f The area percentage and number of thioflavine-S positive fibrillary plaques. g-i Representative bands of Western bolt and densitometry analysis of Aβ1-40 and Aβ1-42 expression levels

in the hippocampus. Data are analyzed by the three-way factor ANOVA with Tukey's post hoc test and represent mean ± SEM from 5 sections per mouse (in c-f) or three independent experiments (in h-i) and four mice per group. *p < 0.05, **p < 0.01, Exercise versus Control; #p < 0.05, ###p < 0.001, APP/PS1 versus WT; &p < 0.05, &&p < 0.01, &&&p < 0.001, AQP4−/−/APP/PS1 versus APP/PS1.

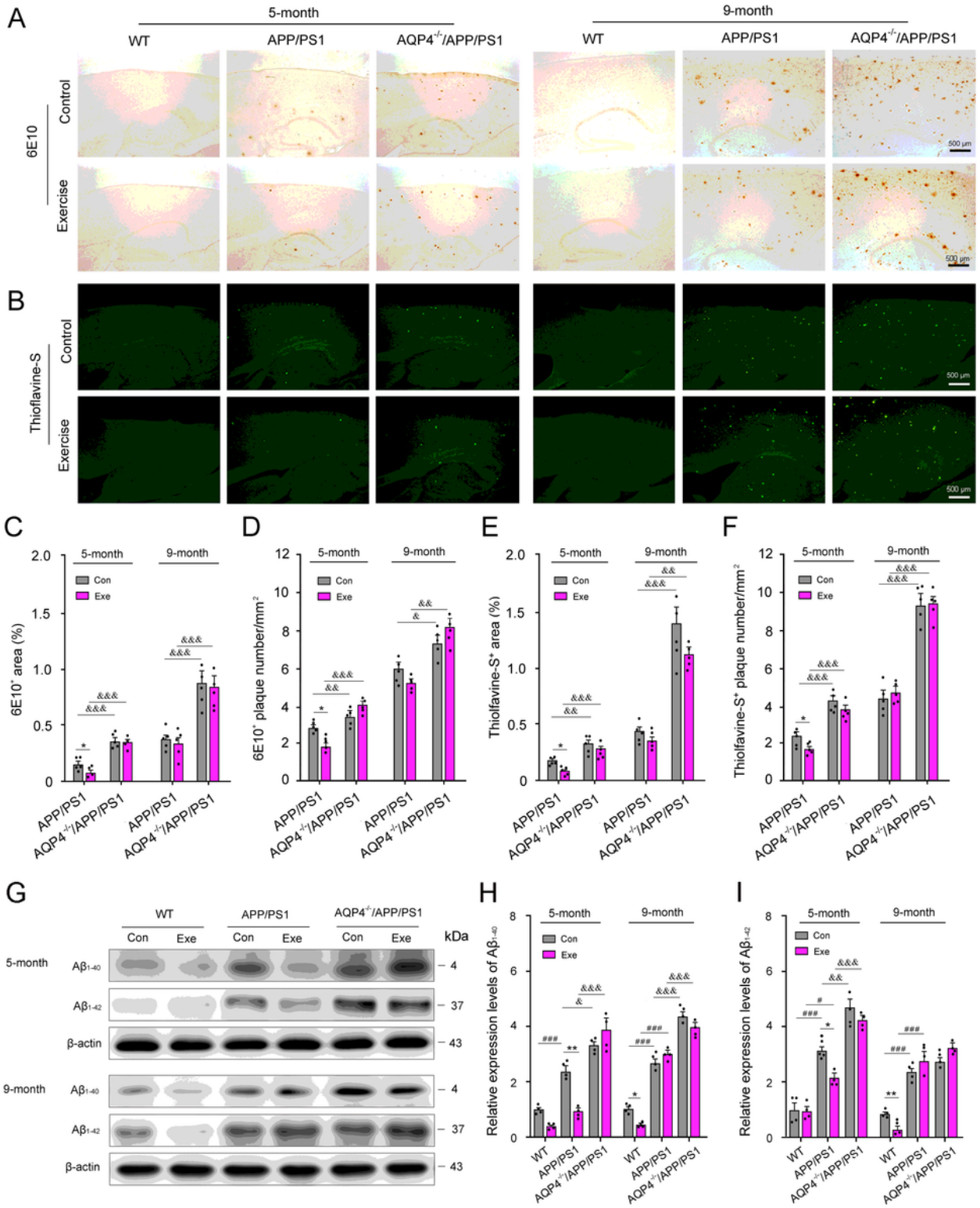

Figure 3

The effect of voluntary exercise on Aβ accumulation in 5- and 9-month-old APP/PS1 mice with or without AQP4. a-b 6E10 immunostaining and thioflavine-S staining showing Aβ plaques in the hippocampus and adjacent cortex, respectively. c-d The area percentage and number of 6E10-immunopositive diffuse plaques. e-f The area percentage and number of thioflavine-S positive fibrillary plaques. g-i Representative bands of Western bolt and densitometry analysis of Aβ1-40 and Aβ1-42 expression levels in the hippocampus. Data are analyzed by the three-way factor ANOVA with Tukey's post hoc test and represent mean ± SEM from 5 sections per mouse (in c-f) or three independent experiments (in h-i) and four mice per group. *p < 0.05, **p < 0.01, Exercise versus Control; #p < 0.05, ###p < 0.001, APP/PS1 versus WT; &p < 0.05, &&p < 0.01, &&&p < 0.001, AQP4−/−/APP/PS1 versus APP/PS1.

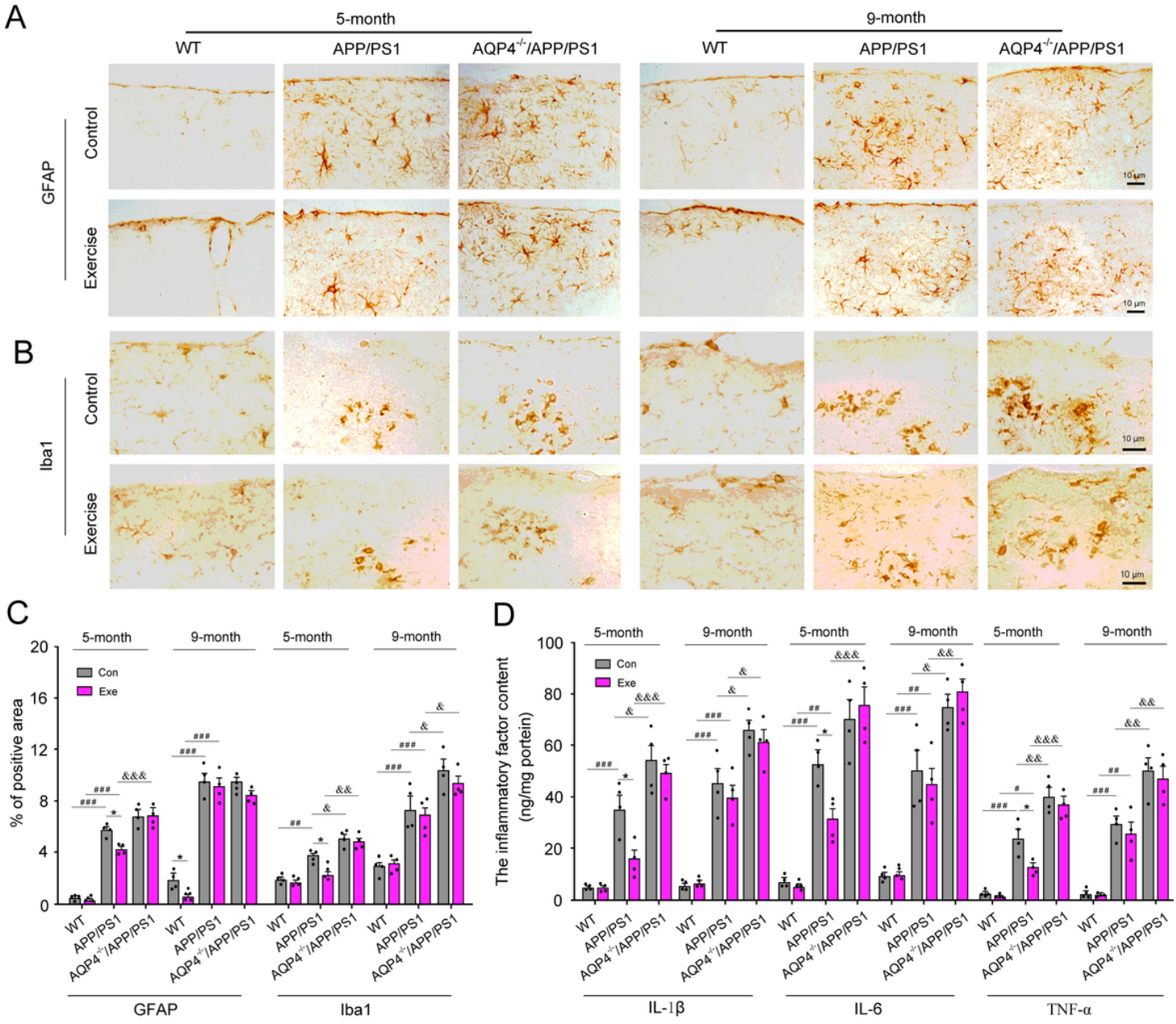

Figure 4

The effect of voluntary exercise on reactive gliosis and inflammatory factor levels in the brain of 5- and 9-month-old APP/PS1 mice with or without AQP4. a-b Immunohistochemical staining for GFAP and Iba1 in

the frontal cortex. c Quantification of the percentage of GFAP and Iba1 positive area in the frontal cortex, respectively. Data represent mean ± SEM from 5 sections per mouse and four mice per group. d ELISA analysis of inflammatory factors IL-1β, IL-6 and TNF-α levels in the frontal cortex. Data represent mean ± SEM from 3 independent experiments and 4 mice per group. Three-way factor ANOVA with Tukey's post hoc test. *p < 0.05, Exercise versus Control; #p < 0.05, ##p < 0.01,###p < 0.001, APP/PS1 versus WT; &p < 0.05, &&p < 0.01, &&&p < 0.001, AQP4−/−/APP/PS1 versus APP/PS1.

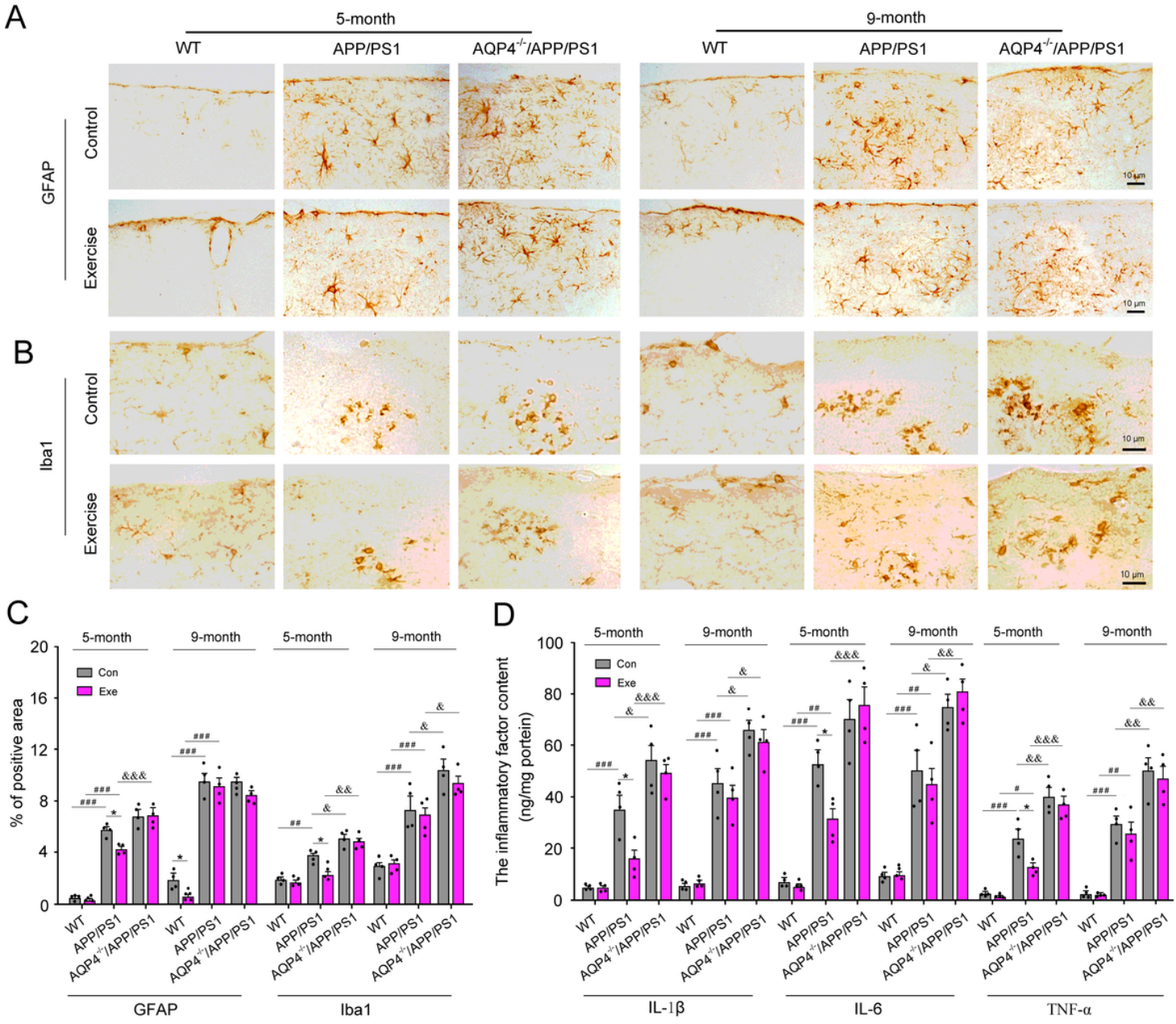

Figure 4

The effect of voluntary exercise on reactive gliosis and inflammatory factor levels in the brain of 5- and 9-month-old APP/PS1 mice with or without AQP4. a-b Immunohistochemical staining for GFAP and Iba1 in the frontal cortex. c Quantification of the percentage of GFAP and Iba1 positive area in the frontal cortex, respectively. Data represent mean ± SEM from 5 sections per mouse and four mice per group. d ELISA analysis of inflammatory factors IL-1β, IL-6 and TNF-α levels in the frontal cortex. Data represent mean ±

SEM from 3 independent experiments and 4 mice per group. Three-way factor ANOVA with Tukey's post hoc test. *p < 0.05, Exercise versus Control; #p < 0.05, ##p < 0.01,###p < 0.001, APP/PS1 versus WT; &p < 0.05, &&p < 0.01, &&&p < 0.001, AQP4−/−/APP/PS1 versus APP/PS1.

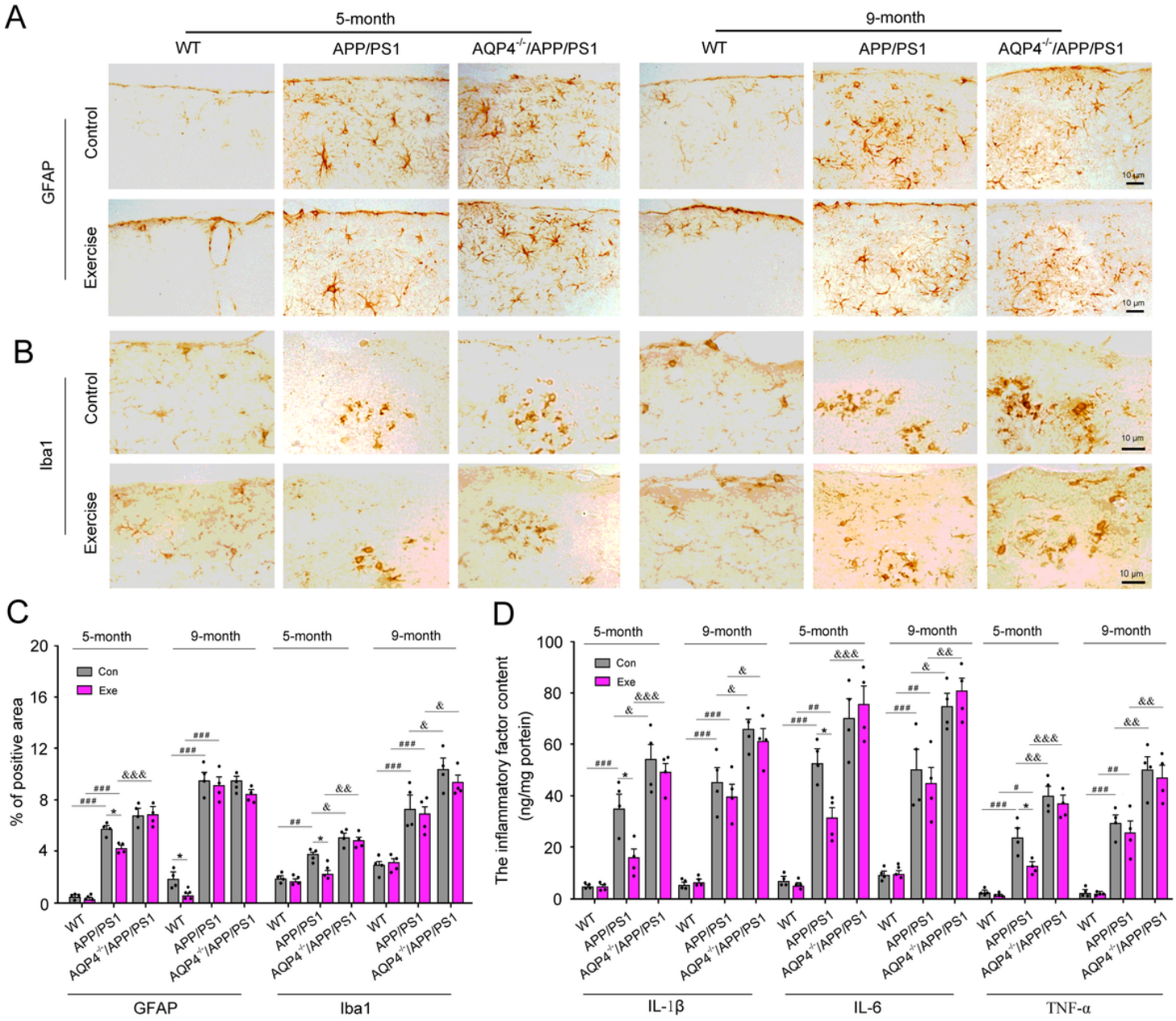

Figure 4

The effect of voluntary exercise on reactive gliosis and inflammatory factor levels in the brain of 5- and 9-month-old APP/PS1 mice with or without AQP4. a-b Immunohistochemical staining for GFAP and Iba1 in the frontal cortex. c Quantification of the percentage of GFAP and Iba1 positive area in the frontal cortex, respectively. Data represent mean ± SEM from 5 sections per mouse and four mice per group. d ELISA analysis of inflammatory factors IL-1β, IL-6 and TNF-α levels in the frontal cortex. Data represent mean ± SEM from 3 independent experiments and 4 mice per group. Three-way factor ANOVA with Tukey's post hoc test. *p < 0.05, Exercise versus Control; #p < 0.05, ##p < 0.01,###p < 0.001, APP/PS1 versus WT; &p < 0.05, &&p < 0.01, &&&p < 0.001, AQP4−/−/APP/PS1 versus APP/PS1.

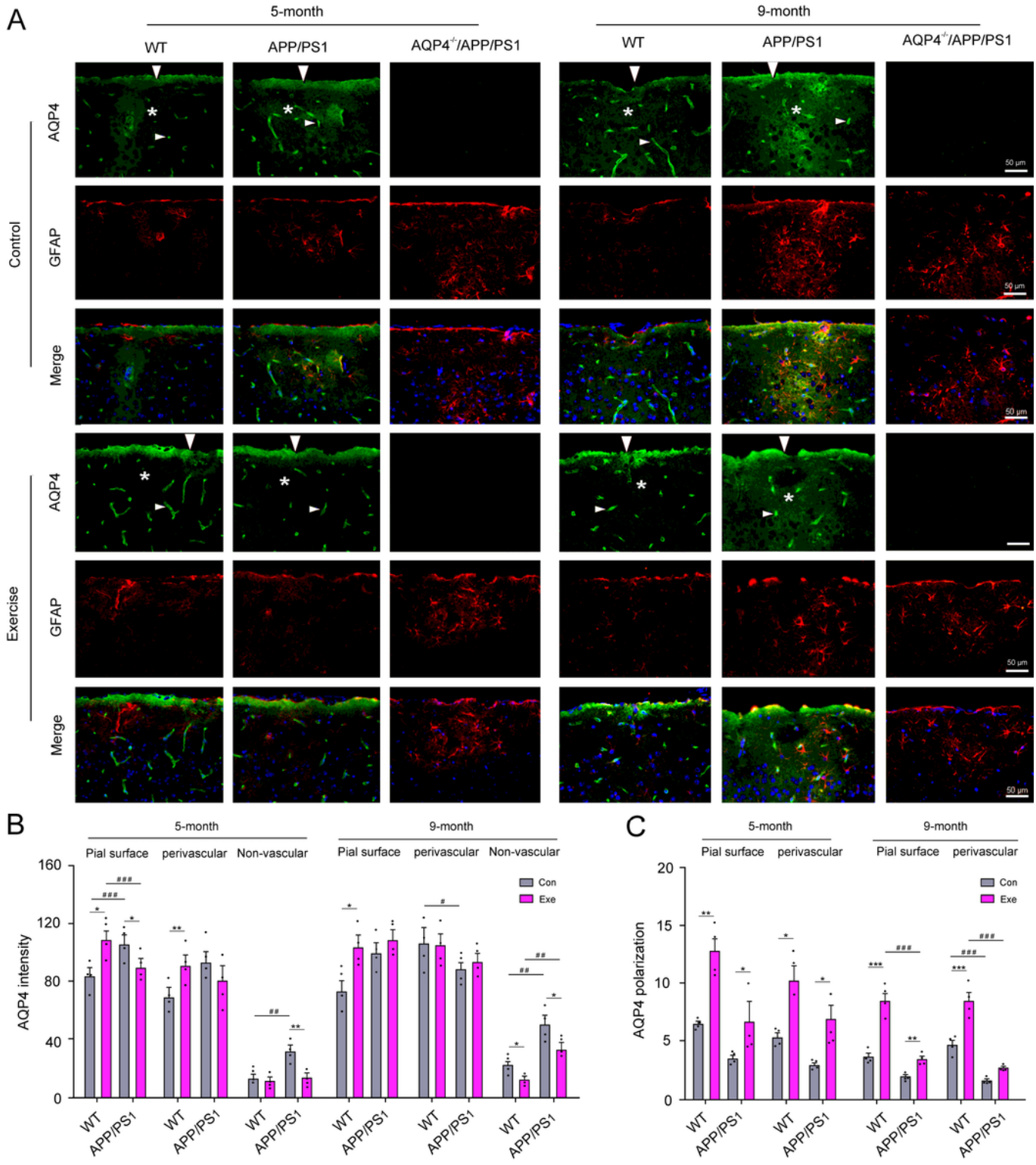

Figure 5

Immunofluorescence staining showing the effect of voluntary exercise on AQP4 expression and polarity in 5- and 9-month-old APP/PS1 mice. a AQP4 and GFAP double immunofluorescence in the frontal cortex. b Quantitative analyses of immunofluorescence intensity of AQP4 at the regions immediately abutting pia maters (large arrowheads) and microvessels (small arrowheads) and as well as correspondingly adjacent parenchymal domains (stars). c Quantitative analyses of AQP4 polarization abutting pia maters

and microvessels. Data are analyzed by the three-way factor ANOVA with Tukey's post hoc test and represent mean ± SEM from 4 sections (16-20 microvessels) per mouse and 4 mice per group. *p < 0.05, **p < 0.01; ***p < 0.001, Exercise versus Control; #p < 0.05, ###p < 0.001, APP/PS1 versus WT.

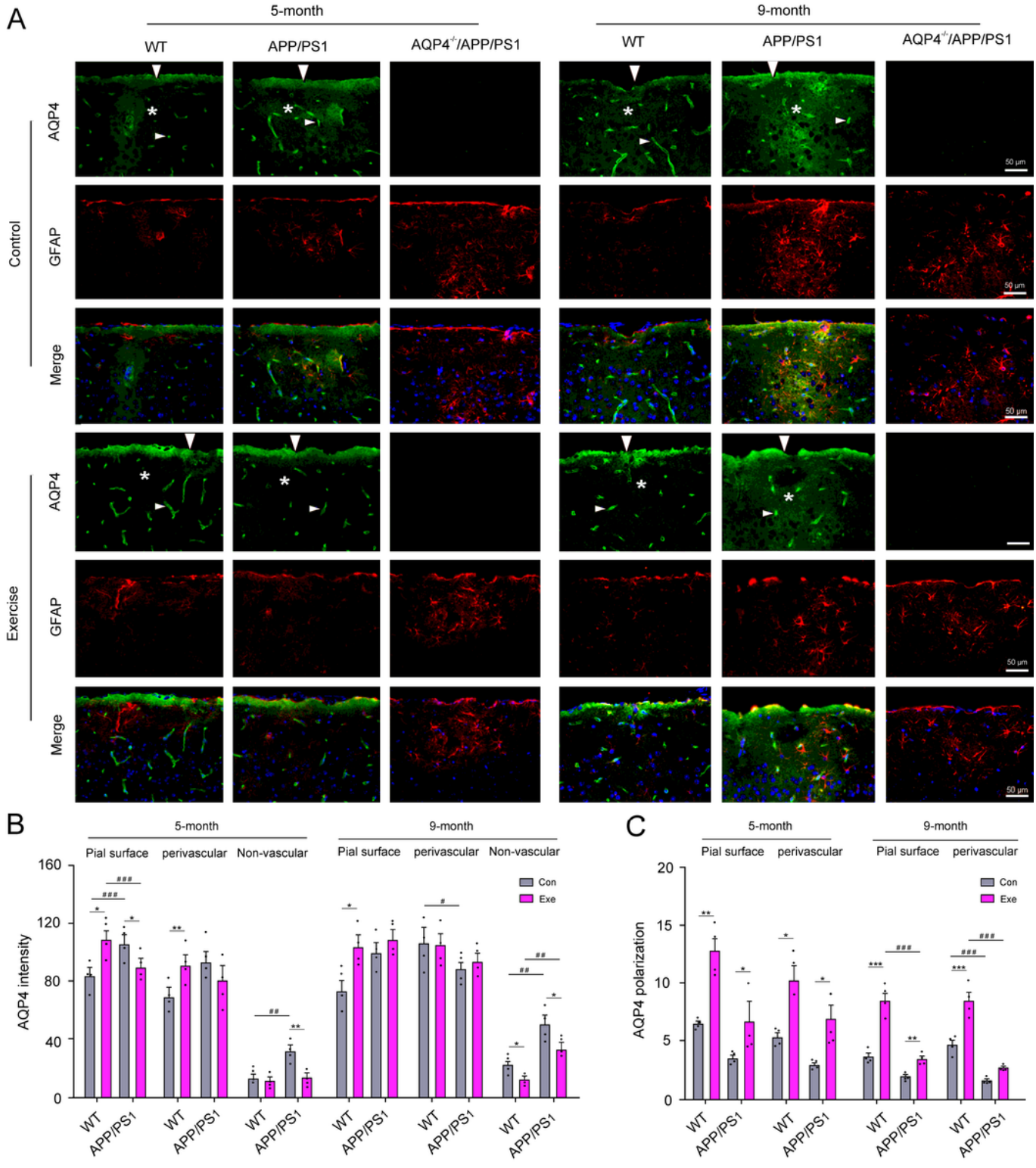

Figure 5

Immunofluorescence staining showing the effect of voluntary exercise on AQP4 expression and polarity in 5- and 9-month-old APP/PS1 mice. a AQP4 and GFAP double immunofluorescence in the frontal cortex.

b Quantitative analyses of immunofluorescence intensity of AQP4 at the regions immediately abutting pia maters (large arrowheads) and microvessels (small arrowheads) and as well as correspondingly adjacent parenchymal domains (stars). c Quantitative analyses of AQP4 polarization abutting pia maters and microvessels. Data are analyzed by the three-way factor ANOVA with Tukey's post hoc test and represent mean ± SEM from 4 sections (16-20 microvessels) per mouse and 4 mice per group. *p < 0.05, **p < 0.01; ***p < 0.001, Exercise versus Control; #p < 0.05, ###p < 0.001, APP/PS1 versus WT.

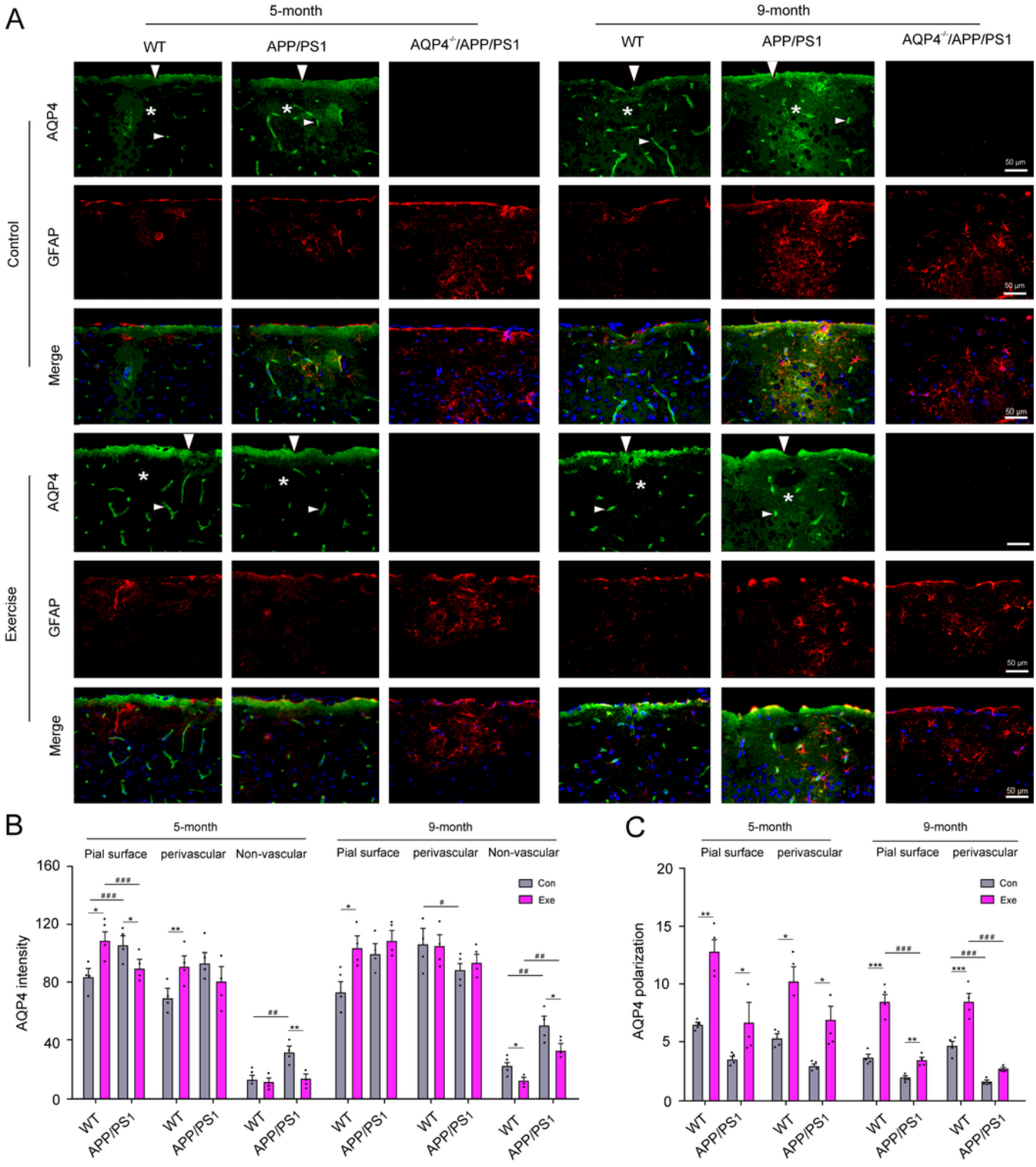

Figure 5

Immunofluorescence staining showing the effect of voluntary exercise on AQP4 expression and polarity in 5- and 9-month-old APP/PS1 mice. a AQP4 and GFAP double immunofluorescence in the frontal cortex. b Quantitative analyses of immunofluorescence intensity of AQP4 at the regions immediately abutting pia maters (large arrowheads) and microvessels (small arrowheads) and as well as correspondingly adjacent parenchymal domains (stars). c Quantitative analyses of AQP4 polarization abutting pia maters and microvessels. Data are analyzed by the three-way factor ANOVA with Tukey's post hoc test and represent mean ± SEM from 4 sections (16-20 microvessels) per mouse and 4 mice per group. *p < 0.05, **p < 0.01; ***p < 0.001, Exercise versus Control; #p < 0.05, ###p < 0.001, APP/PS1 versus WT.

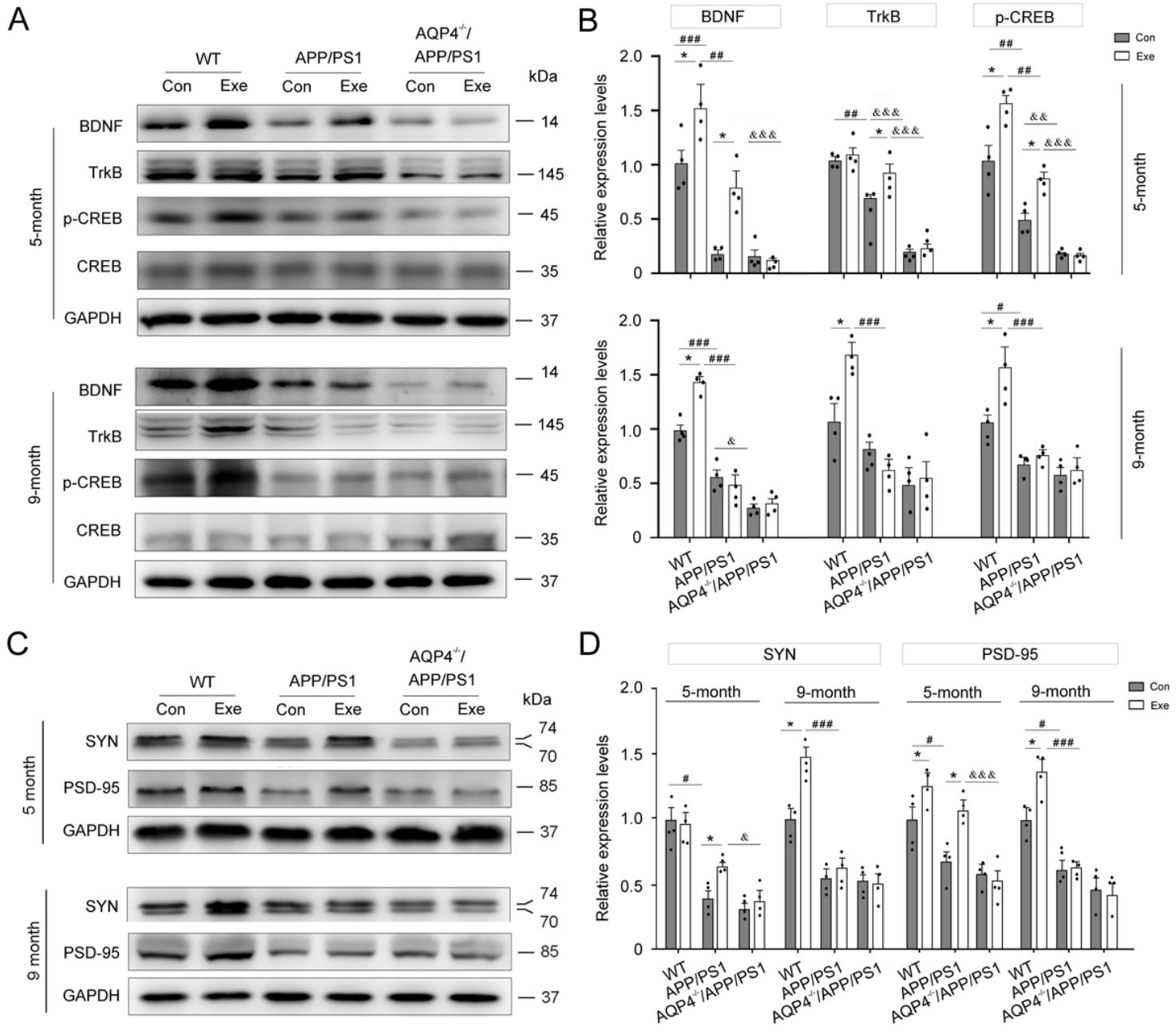

Figure 6

The effect of voluntary exercise on BDNF-TrkB signaling activation and synaptic protein levels in the brain of 5- and 9-month-old APP/PS1 mice with or without AQP4. a-b Representative bands of Western

blot and densitometry analysis of BDNF, TrkB and p-CREB levels. c-d Representative bands of Western bolt and densitometry analysis of SYN and PSD-95 expression levels in the hippocampus. Data are analyzed by the three-way factor ANOVA with Tukey's post hoc test and represent mean ± SEM from 3 independent experiments and 4 mice per group. *p < 0.05, Exercise versus Control; #p < 0.05, ##p < 0.01, ###p < 0.001, APP/PS1 versus WT; &p < 0.05, &&p < 0.01, &&&p < 0.001, AQP4−/−/APP/PS1 versus APP/PS1.

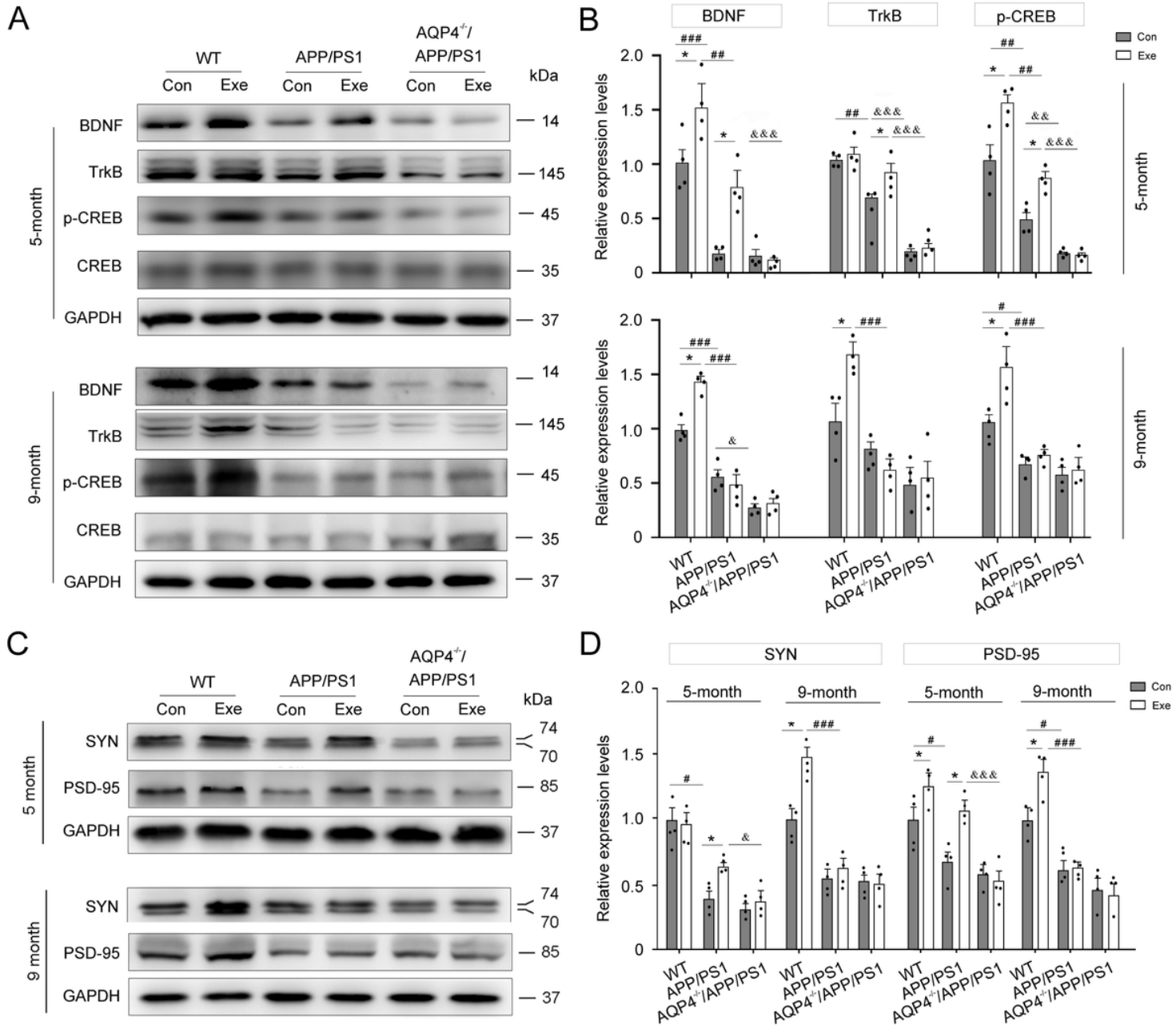

Figure 6

The effect of voluntary exercise on BDNF-TrkB signaling activation and synaptic protein levels in the brain of 5- and 9-month-old APP/PS1 mice with or without AQP4. a-b Representative bands of Western blot and densitometry analysis of BDNF, TrkB and p-CREB levels. c-d Representative bands of Western bolt and densitometry analysis of SYN and PSD-95 expression levels in the hippocampus. Data are

analyzed by the three-way factor ANOVA with Tukey's post hoc test and represent mean ± SEM from 3 independent experiments and 4 mice per group. *p < 0.05, Exercise versus Control; #p < 0.05, ##p < 0.01, ###p < 0.001, APP/PS1 versus WT; &p < 0.05, &&p < 0.01, &&&p < 0.001, AQP4−/−/APP/PS1 versus APP/PS1.

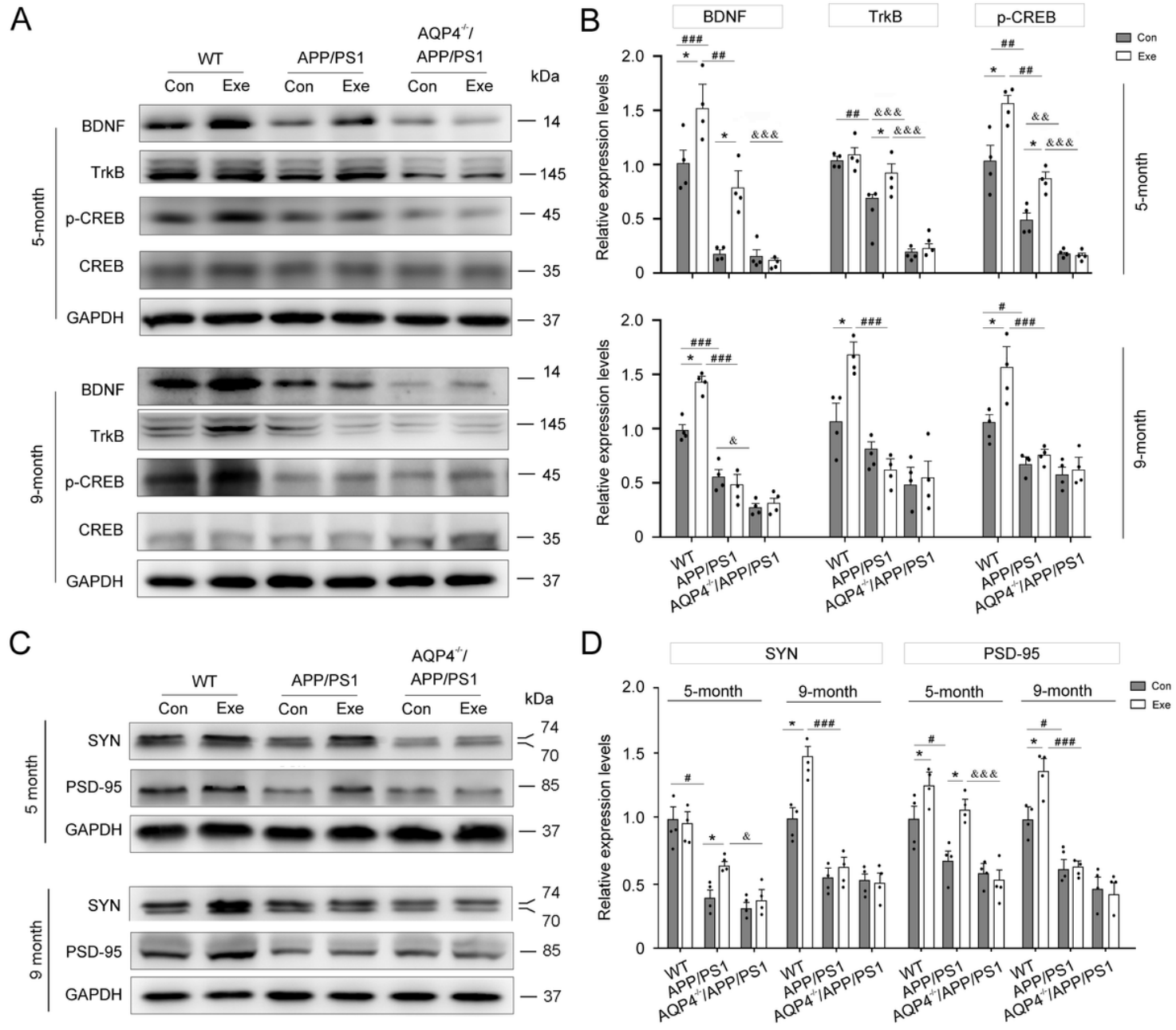

Figure 6

The effect of voluntary exercise on BDNF-TrkB signaling activation and synaptic protein levels in the brain of 5- and 9-month-old APP/PS1 mice with or without AQP4. a-b Representative bands of Western blot and densitometry analysis of BDNF, TrkB and p-CREB levels. c-d Representative bands of Western bolt and densitometry analysis of SYN and PSD-95 expression levels in the hippocampus. Data are analyzed by the three-way factor ANOVA with Tukey's post hoc test and represent mean ± SEM from 3 independent experiments and 4 mice per group. *p < 0.05, Exercise versus Control; #p < 0.05, ##p < 0.01,

###p < 0.001, APP/PS1 versus WT; &p < 0.05, &&p < 0.01, &&&p < 0.001, AQP4−/−/APP/PS1 versus APP/PS1.

Supplementary Files

This is a list of supplementary files associated with this preprint. Click to download.

- FigureS1.tif
- FigureS1.tif
- FigureS1.tif
- FigureS2.tif
- FigureS2.tif
- FigureS2.tif
- FigureS3.tif
- FigureS3.tif
- FigureS3.tif
- FigureS4.tif
- FigureS4.tif
- FigureS4.tif